Magnetoimpurity Resonances in Semiconductor Transport

V.F. GANTMAKHER and V.N. ZVEREV

Institute of Solid State Physics, Academy of Sciences of the USSR
Chernogolovka, USSR

Contents

1. Introduction

In this chapter we discuss the manifestation of the resonant interaction of free carriers and shallow impurity centers in magnetotransport phenomena. First of all, we mean by this inelastic interactions, i.e., transitions involving, one way or another, free carriers: inelastic scattering, impact ionization or photoionization, recombination, etc. The probability of such processes depends on the density of initial and/or final states of free carriers taking part in transitions. In strong magnetic fields the density of states is nonmonotonic. It has sharp maxima near the bottom of magnetic subbands, separated by cyclotron energy which depends on the magnetic field B. Hence, the resonant dependences of transition probabilities on the magnetic field follow, giving rise to extrema in the transport properties.

In principle, resonances in elastic scattering may also occur if the probability of such scattering by a center changes for some reasons in a resonant way with magnetic field.

Though the magnetoimpurity resonances have already been observed in about a dozen of semiconductors there is only one brief review by Eaves and Portal (1979) dealing with the subject. In the present chapter we try to fill up the gap.

In the two sections (2 and 3) we classify magnetoimpurity resonances and analyze energy relations which govern them. This analysis demands accounting for the effect of the magnetic field on the impurity spectrum, quasibound Coulomb states below the Landau levels, nonparabolicity of the free carrier dispersion law. In addition, we discuss the direction of resonant transitions. Under nonequilibrium conditions this problem proves often to be nontrivial. For example, in inelastic scattering of a free carrier by a neutral impurity center, the same resonance condition describes both cooling of a hot electron accompanied by center excitation as well as center de-excitation with energy transfer to the carrier.

In the remaining sections we deal with the manifestation of the magneto-impurity resonances in the transport properties. In all known cases these resonances have been observed under nonequilibrium conditions, i.e., either with photoexcited carriers, or with carriers heated by the electric field. We shall not go into experimental details in this chapter, referring readers to original papers by Eaves et al. (1974) and Gantmakher and Zverev (1975).

In section 4 we discuss how the resonant transitions do affect the transport properties. Though the relative variation of the magnetoresistance in the resonance can be of the order of unity, it is often difficult to make out whether it is related to changes in the mobility of the free carriers, or to changes in their number. These difficulties are, in the first place, conditioned by the multicomponent character of the excited system. We shall consider here only the simplest cases yielding to analysis, i.e., n-Ge and n-GaAs under far-infrared photoexcitation.

The last section deals with the inversion of the magnetoimpurity resonances. When the system is shifted too far from the equilibrium by intense photo-excitation, by a heating electric field or owing to a too low temperature of the bath, the response to the resonance may change its sign, i.e., magneto-resistance maxima may give way to minima at the same values of the magnetic field. This phenomenon appears to be rather common in the nonequilibrium semiconductors. It was also observed while studying the magnetophonon resonance on hot carriers (Aksel'rod et al. 1969) and of the conductivity response to the cyclotron resonance (Gershenzon et al. 1968). It also manifests itself in spectra of photocurrent induced by monochromatic excitation (Protasov and Rodionov 1974). Therefore the contents of this section can be useful also in reference to other domains of physics of hot electrons.

2. Classification of transitions

In a strong magnetic field B, when the condition

$$\Omega\tau \gg 1$$

is satisfied ($\Omega = eB/m_c c$ is the cyclotron frequency of electrons, m_c is the cyclotron mass, τ is the momentum relaxation time) the spectrum of the free carriers is split into a series of one-dimensional magnetic subbands and, spin neglected, has the form

$$E = E_n + \hbar^2 k_\parallel^2/2m_\parallel, \qquad n = 0, 1, 2, \ldots,$$

where the sequence E_n is the Landau level energies, $k_\parallel$ is the longitudinal wavevector, the mass $m_\parallel$ characterizes translational motion along B. The energy dependence of the density of states has a singularity at the bottom of each magnetic subband. In a simple parabolic band the Landau levels are equidistant:

$$E_n = \hbar\Omega(n + \tfrac{1}{2}). \tag{1}$$

Here and below the energy is measured with respect to the band edge at $B = 0$.

The energy spectrum of a shallow Coulomb center in the magnetic field (fig. 1) also undergoes significant changes [see, for example, the review by Bassani et al. (1974)]. If the magnetic field is weak, i.e., if $\hbar\Omega \ll \mathrm{Ry}^*$ ($\mathrm{Ry}^* = me^4/(2\hbar^2\kappa^2)$ is the effective Rydberg energy, κ is the dielectric constant), its effect can be accounted for by the perturbation theory. The analytic solution of this problem gives the Zeeman splitting of impurity levels linear in field and the diamagnetic shift quadratic in field. In the intermediate fields ($\hbar\Omega \approx \mathrm{Ry}^*$) there is no exact solution and variational calculations are usually used. In the strong field limit

$$\hbar\Omega \gg \mathrm{Ry}^* \tag{2}$$

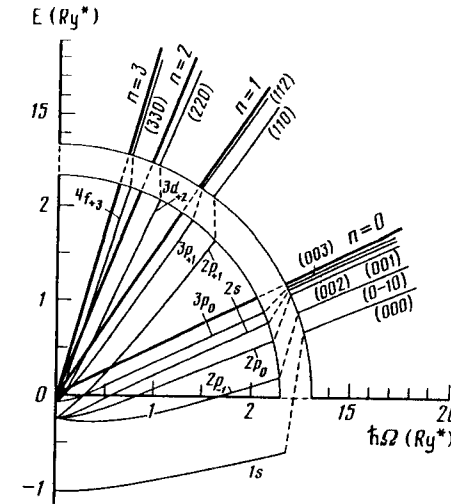the Coulomb energy can be considered small in comparison with the cyclotron

Fig. 1. Energy spectrum of a hydrogen-like Coulomb center, in a magnetic field.

energy, and the problem can again be solved analytically in the so-called adiabatic approximation. In this approximation the typical size of the wave function in the plane perpendicular to the field is considered to be much smaller than along the field.

In a magnetic subband the states are characterized by their number n and the component m of the orbital moment ($n \geq m > -\infty$). In the strong field limit under each subband a sequence of levels of the Coulomb center arises with energies given by

$$E_{nm\mu} = E_n + \varepsilon_{nm\mu}, \qquad \mu = 0, 1, 2, \ldots, \qquad \varepsilon_{nm\mu} < 0. \tag{3}$$

Here we use the notation of Coloumb levels after Boyle and Howard (1961). The sequence (3) converges to the Landau level E_n. The correspondence between the levels (3) and the initial spectrum of a hydrogen-like center in the absence of a field can be established without tracing the field dependence of $E_{nm\mu}$. It is sufficient to use the rule of noncrossing of levels with the same symmetry (i.e., with the same values of m and the same parity) with B changing, the known spectrum in weak magnetic field and the theorem about alternation of state parity in a one-dimensional potential well. Such correspondence for a number of levels is shown in fig. 1.

The levels of a hydrogen-like center with $m \leq 0$ all fall below the lowest magnetic subband. The states of the initial spectrum with $m > 0$ in a strong field fall below the Landau levels with $n = m$ forming a sequence of levels ($m\,m\,u$) with $\mu = 0, 1, \ldots$. These states are stable since they have no symmetry counterparts in

the lower magnetic subbands. In contrast with them, the states with $m < n$ at $n > 0$ are, strictly speaking, quasidiscrete and decay into a continuum due to inaccuracy of the adiabatic approximation.

The larger the wave function of a bound Coulomb state the stronger will be the effect of the magnetic field on it. Therefore, the adiabatic approximation for different states is valid, beginning with different values of B. As shown by Gel'mont and Efros [see Gantmakher et al. (1983)] in the quasiclassical region ($n \gg 1$) the adiabatic approximation is valid, if a less rigid condition than that given by eq. (2) is satisfied:

$$n\hbar\Omega \gg \text{Ry}^*, \tag{4}$$

i.e., the main features of the quasibound Coulomb state spectrum appear in the quasiclassical region in relatively weak magnetic fields, for which $\hbar\Omega \lesssim \text{Ry}^*$. In fig. 1 the adiabatic approximation is valid in the region situated outside the outer circumference.

In fig. 2 which shows schematically the electron spectrum in a magnetic field in the vicinity of a shallow Coulomb center the states are sorted into bound (b), quasibound (qb) and free (f) groups. Arrows indicate various transitions in this spectrum.

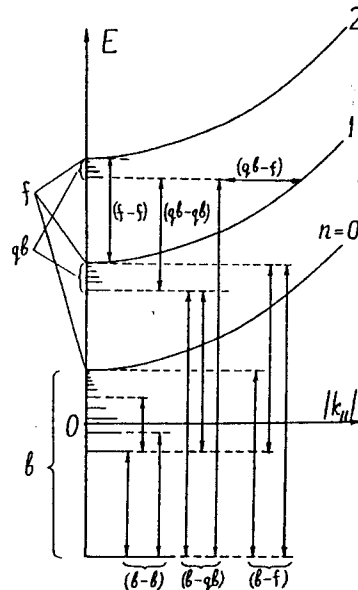The transitions between b-states accompanied by the interaction of the

Fig. 2. Transitions between the bound (b), quasibound (qb) and free (f) states of an electron in the magnetic field.

impurity with a photon or a phonon are studied by magnetooptics and magnetopiezospectroscopy, and generally speaking, are beyond the scope of this chapter. However, these very transitions, but accompanied by inelastic scattering of a free electron, determine the most widespread magnetoimpurity resonances. They are discussed in section 3.1. The b–b transitions play also an important role in the occurrence of resonances in the magnetoresistance of tellurium (von Klitzing 1978), though the origin of the resonances in this case is different (see section 3.6).

The b–f transitions are of two kinds: ionization of the impurity and capture of a free carrier by the center. Experimental data concerning b–f transitions accompanied by inelastic scattering of free carriers are gathered in section 3.2. Note that transitions of this type but with energy transfer to photons can be important only in the weak magnetic field limit (Wallis and Bowlden 1958, Hasegawa and Howard 1961).

Usually, the process of impurity ionization has an intermediate stage in the strong magnetic field: a b–qb transition occurs first, followed by an elastic qb–f transition. The former has a resonant character, and therefore these processes are within the scope of this chapter (see section 3.4). The reverse processes of resonant capture are discussed in section 3.5.

In the strong field limit due to inequality (2) the energy difference between Coulomb states, belonging to different Landau levels, is close to the energy difference between the Landau levels themselves. For example, in n-InSb due to the smallness of the electron effective mass the strong field limit is easily achieved in experiments; then the transitions of the b–qb type manifest themselves as satellites of the cyclotron resonance line (see the contribution by Otsuka in this volume).

Figure 2 includes also f–f transitions (cyclotron or magnetophonon resonances involving carrier interaction with photons and phonons, respectively) and qb–qb transitions (the same resonances but occurring in the vicinity of the impurity). One can hardly expect to be able to distinguish experimentally these two types of transitions. However, it is just f–f transitions that participate in the magnetoimpurity resonances of inelastic scattering described in section 3.1. Apart from inelastic, also elastic f–f transitions, both, intrasubband and intersubband, are possible. They should be pictured by horizontal arrows but are omitted in fig. 2.

Both band anisotropy and degeneracy complicate the spectrum of Coulomb states significantly. For example, in the valence band of germanium qb-states below the light hole Landau levels are formed basically by the wave functions of light holes. The energy $\hbar\Omega_\ell$ becomes of the order of the energy Ry^*_ℓ in the field $B \approx 1$ T. Therefore with respect to this part of the spectrum the fields of 5–10 T are strong. However, for b-states under the lowest magnetic subband formed mainly by the wave functions of heavy holes such fields are still weak in the sense that the Zeeman splitting of low-lying states of an acceptor is significantly

smaller than its ionization energy E_{ion}. Strictly speaking, the spectrum shown in fig. 2 is related just to this case.

Spectra containing b- and qb-states in the magnetic field can arise also in the vicinity of short-range attracting centers. The role of such centers can be played, for example, by shallow neutral impurities, capturing carriers to form the so-called H⁻ centers. According to Andreev (1978), the spectrum of such a center in a magnetic field is qualitatively similar to the spectrum of a hydrogen-like impurity, so that the classification of different types of transitions made above can also be applied to these centers.

3. Resonance relations

3.1. Inelastic scattering

Due to the existence of maxima in the density of states near the bottom of magnetic subbands, most of the free carriers in the semiconductor in a sufficiently strong magnetic field are near the bottom of the subband. Then a resonance is possible for inelastic scattering processes with the energy transfer ΔE fixed by the properties of the scattering center. If the relation

$$N\hbar\Omega = \Delta E, \qquad N = \Delta n = 1, 2, ..., \tag{5}$$

is satisfied, then transitions are possible from the bottom of one subband (where electrons are located) to the bottom of another, and the large density of final states increases the probability of inelastic scattering. While B is changing, eq. (5) becomes valid successively for different N. The values of resonant magnetic fields are arranged periodically in the reciprocal field scale with the period

$$\Delta(1/B) = P = e\hbar/m_c c\Delta E. \tag{6}$$

Rigorous calculation of the probability W_{ie} of inelastic electron scattering by impurities in a magnetic field is a complicated problem, since the transition matrix element M_{ie} is expressed through integrals of poorly known wave functions of the ground and excited states of the impurity in a strong magnetic field. We can only assert that the B-dependence of M_{ie} is comparatively weak and monotonic. Hence, changes in W_{ie} near the resonance are mainly related to the density of final states of free carriers in a magnetic subband $g_n(E) \propto (E - E_n)^{-1/2}$ and all transport parameters of the sample are oscillating periodically in the reciprocal field.

Resonant inelastic scattering of this type has been observed in n-GaAs (Hoult 1974, Eaves et al. 1974, Nicholas and Stradling 1976, Zverev 1983, Zverev and Shovkun 1984a), n-Ge (Instone et al. 1977, Zverev and Shovkun 1984b) and Te (von Klitzing 1978) in magnetoresistance measurements both in non-ohmic regimes and under photoexcitation conditions. Resonances in photoexcited

p-Ge (Gantmakher and Zverev 1975, 1976a, Instone et al. 1977) were considered for a long time to be brought about by the same processes. In fact, they are of a different origin, which will be discussed in section 3.3.

Experimental curves in fig. 3 demonstrate the resonant inelastic scattering of carriers heated by electric field (Hoult 1974). The positions of the extrema in the series Y are given by eq. (5) with the transferred energy ΔE equal to the lowest excitation potential of a shallow donor.

In most of the experiments, the observed resonances are caused by transitions between the lowest of the excited states and the ground state (the reasons why just this transition is distinguished from the others will be discussed later). Now and then, other resonant transitions are also observed. For example, in photoexcited n-GaAs the main series of magnetoimpurity oscillations is determined by the inelastic scattering of electrons by donors with an energy transfer ΔE which equals the lowest excitation potential of the donor. However, apart from this main series, additional resonances are seen in the lower curve in fig. 4 brought about by transitions involving several higher-lying excited states. These additional resonances are shown in detail in the inset, where the region of large magnetic fields is shown on an extended linear, instead of reciprocal, scale.

Experiments on n-GaAs demonstrate the ability of the magnetoimpurity resonances to give information about the energy spectrum of a shallow impurity. Note that by means of this simple technique, without a spectral instrument, a relatively high resolution can be achieved [see also fig. 9, taken from the paper of Nicholas and Stradling (1978)].
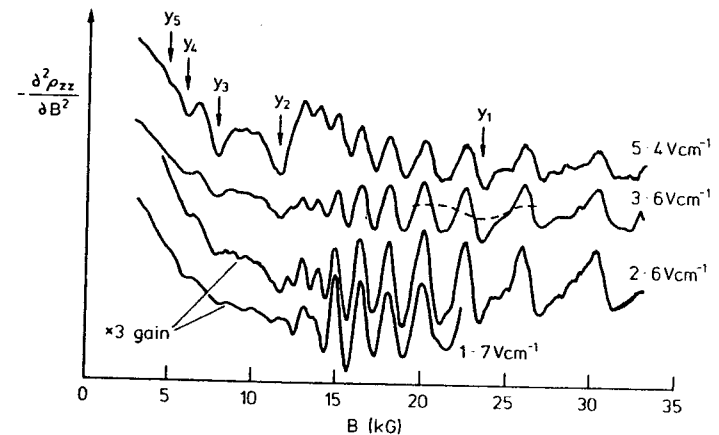

Fig. 3. Magnetoimpurity resonances in the non-ohmic longitudinal magnetoresistance of n-GaAs. The series Y is due to inelastic scattering, the series of smaller period is conditioned by the resonant capture of electrons by impurity, assisted by LO-phonon emission (see section 3.5) (after Hoult 1974).
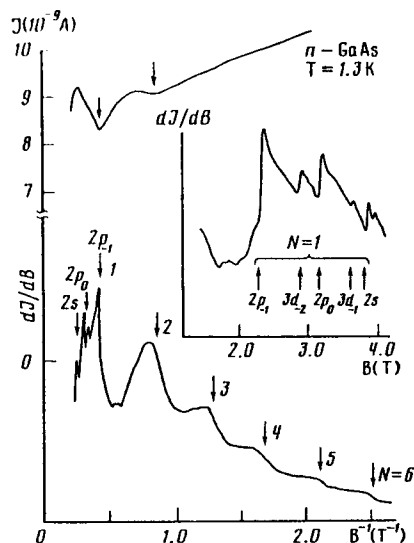
Fig. 4. Magnetoimpurity resonances of the inelastic scattering in photoconductivity of n-GaAs. The arrows indicate the calculated values of the resonant fields (after Zverev and Shovkun 1984a).

The B dependence of the energy ΔE, entering eq. (5), affects the values of resonant fields and their period in the reciprocal field. Expanding ΔE in a series in B, we get

$$\Delta E(B) \approx \Delta E(0)(1 + aB + bB^2). \qquad (7)$$

Substituting eq. (7) into eq. (5) and dividing both sides of the equation by $B \Delta E(0)$, we obtain

$$PN = B_N^{-1} + a + bB_N. \qquad (8)$$

As seen from eq. (8), the linear term in $\Delta E(B)$, e.g., conditioned by the Zeeman splitting, does not affect the periodicity, leading only to a phase shift. The violation of periodicity in B^{-1} is due only to the quadratic term.

Figure 5 shows the N dependence of the reciprocal resonant fields B_N^{-1} in photoexcited n-GaAs obtained from fitting the curves shown in fig. 4. The resonant fields corresponded to minima of the dependence $J(H^{-1})$ and to steep parts of the function dJ/dB on the field. The slope of the straight line in fig. 5 determines the period of oscillations, yielding according to eq. (6) the transferred energy $\Delta E \approx 4.2$ meV. This value is close to the lowest excitation potential of donors in GaAs $E_{01} \approx \frac{3}{4} E_{ion} \approx 4.29$ meV.

The measurements of the period can be considered as a starting point in the treatment of the experimental data. However, one should remember that
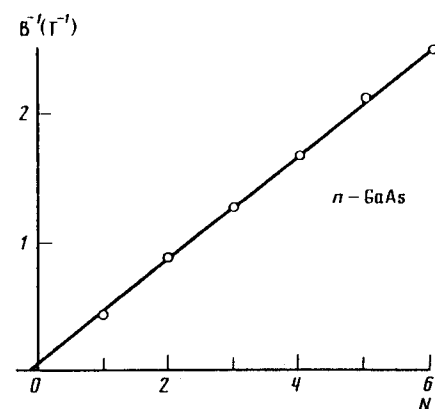
Fig. 5. The periodicity of the main series of magnetoimpurity resonances in n-GaAs, shown in fig. 4.

nonlinearity of the field dependence of ΔE can appreciably decrease the accuracy of the determination of $\Delta E(0)$.

If the field dependence of ΔE is known rather well it can be accounted for by direct substitution into eq. (5). For example, in fig. 1 the dependence on B of the energy of low-lying states of a hydrogen-like center is shown, calculated by Aldrich and Greene (1979) by the variational method. It gives with great accuracy the excitation spectrum of a shallow impurity near the edge of a simple band with an isotropic carrier spectrum, i.e., it can be applied, for example, to shallow donors in A^3B^5 semiconductors. To obtain ΔE, however, one needs also the experimental values of the ground state chemical shift. The resonant fields calculated for GaAs, with this shift taken into account, are marked in fig. 4 by arrows.

3.1.1. Direction of the energy transfer

The resonant condition (5) describes two opposite processes: carriers cooling accompanied by excitation of centers and de-excitation of centers with energy transfer to carriers. Under thermal equilibrium, when the rates of both processes are the same, their contribution to the transport phenomena is relatively small. At $kT \ll E_{ion}$ the number of excited impurities is exponentially small, the same as the number of free carriers capable to excite or to ionize an impurity. With the temperature increased, the number of electrons with energies $E \gtrsim E_{ion}$ and the population of excited levels increase, but still both remain exponentially small, when, due to a high statistic factor of the band, a significant part of the impurities is already thermally ionized. This accounts for the absence of experiments, in which the inelastic electron scattering by impurities is observed under equilibrium conditions.

In the presence of a heating electric field or photoexcitation, the state of the

electron system is far from equilibrium. The number of excited impurities and the number of hot electrons become appreciably higher than their equilibrium values. As a result, inelastic electron–impurity scattering increases and makes a perceptible contribution to the transport properties of the system of non-equilibrium carriers, and the resonances in this scattering are revealed in the experiment. However, the question of a dominant direction of transitions immediately arises.

There are several experimental approaches to the problem. One of them consists of measuring the coefficient β, characterizing the deviation of the hot-electron mobility μ from the ohmic mobility μ_0 (Hamagushi et al. 1972):

$$\mu = \mu_0(1 - \beta\mathscr{E}^2),\qquad(9)$$

where $\mathscr{E}$ is the applied electric field, β is proportional to the constant α which relates changes in effective electron temperature T_e with the square of electric field,

$$T_e - T = \alpha\mathscr{E}^2.$$

The value of β is determined by measuring the voltage V_3 of the third harmonic at a fixed amplitude of the alternating current which feeds the sample. The form of resonant lines on the β versus B curve allows one to determine the sign of energy variation in the electron system at resonance. This method has been applied to magnetoimpurity resonances by Nicholas and Stradling (1976, 1978). They have shown that the resonance corresponds to maxima in the warm electron coefficient β and hence to heating of the free carriers through the de-excitation of the donors.

3.1.2. Intracenter energy relaxation

The lowest excited state is distinguished from the other states due to the specific character of the intracenter energy relaxation process. An ionized center is known to capture a nonequilibrium carrier into a highly excited state; then it drops by emitting acoustic phonons. Therefore under stationary conditions the population of the ith excited state is proportional to its lifetime τ_i^{ph} with respect to phonon emission. The probability of acoustic phonon emission by hydrogen-like centers in semiconductors is governed by a parameter qa^*, where q is the wavevector of the emitted phonon, a^* is the effective size of the center (Ascarelli and Rodriguez 1961, Brown and Rodriguez 1967). When the excited center relaxes, the most probable transitions are those for which $qa^* \approx 1$. At small values of qa^* this probability is low due to the small phase volume for phonons to be emitted, and at large qa^*, due to the phonon wavelength being much smaller than the size of the impurity center. The transitions with $qa^* \approx 1$ ensure the electron to descend comparatively quickly to the lowest excited state. The transition to the ground state is, however, difficult since for this last step $qa^* \gg 1$. For example, the probability of the phonon-assisted transition $2s \to 1s$ in the

hydrogen-like center is 170 times smaller than the probability of the $3s \to 2s$ transition (Meshkov 1979).

It is a rather general statement that the transition to the ground state is characterized by a large value of the parameter qa^* (Meshkov and Rashba 1979). The transition energy ΔE is of the order of the center ionization energy

$$\Delta E \approx E_{ion} \approx e^2/\kappa a^*,$$

and therefore

$$qa^* \approx (\Delta E/\hbar s)a^* \approx e^2/\kappa\hbar s \equiv \alpha^*,$$

where s is the sound velocity. The effective 'fine structure constant' α^* depends weakly on band parameters and is large for most of the semiconductors: $\alpha^* \approx 30 \gg 1$. Inequality $qa^* \gg 1$ is valid also for acceptors in cubic semiconductors with a degenerate valence band, when the transition to the ground state is assumed.

Generally speaking, the magnetic field changes the probability of intracenter transitions. In strong fields the effective size of wave functions of impurity bound states in the direction perpendicular to B diminishes, leading to a decreased parameter qa^* and to an increased probability of transitions with phonon emission (Perel' and Polyakov 1981). However this effect is important only if $\hbar\Omega \gg Ry^*$, i.e., in the limit which is 'ultraquantum' for magnetoimpurity resonances of inelastic scattering.

Therefore, we are more interested in the opposite effect in weaker fields. A magnetic field removes degeneracy and splits center levels. As a result, the symmetry of the lowest excited state may change. For example, the levels of the hydrogen-like center split in a magnetic field so that the lowest excited state is $2p_-$, while the split-off 2s-state shifts upwards (fig. 1).

The probability of spontaneous phonon emission is proportional to the factor $(qa^*)^{-2(l_1+l_2)}$, i.e., it depends on orbital quantum numbers l_i of the levels involved in the transition (Ascarelli and Rodriguez 1961). Therefore the lifetime of the lowest excited state of the hydrogen-like center in a magnetic field increases $(qa^*)^2$ times, when the Zeeman splitting of this state becomes larger than kT. The estimates show that the lifetime τ^{ph} of excited donors in GaAs in a magnetic field becomes of the order of 10^{-4} s.

As a matter of fact, the existence of only one period of oscillations determined by the energy transfer $\Delta E = E_{01}$, which is equal to the lowest excitation potential of the impurity, is in itself an experimental evidence of impurity de-excitation being the dominating process. For the opposite process, i.e., for the excitation of impurities by hot electrons, there are no physical reasons for which one of the excited states would be distinguished.

Additional resonances in strong field in photoexcited n-GaAs (fig. 4) can also be explained in the framework of the model based upon the long lifetime of the lowest excited state (see section 4).

3.1.3. Anisotropic centers

Relaxation of the impurity center in a material with a highly anisotropic energy band has some specific features. Consider, for example, donors in Ge. Due to a high anisotropy of the effective electron mass, the wave functions of donors appear to be compressed in the heavy mass direction. Therefore, there exists a direction of phonon emission which is characterized by a smaller qa^* value than in the isotropic case. As a result, the lifetime of the donor's lowest excited state becomes of the order of the lifetimes of higher excited states, being two orders of magnitude smaller than that in an acceptor in Ge (Meshkov 1979). In experiments on n-Ge under conditions of interband (Instone et al. 1977) as well as impurity (Zverev and Shovkun 1984b) photoexcitation, those magnetoimpurity resonances were observed which corresponded to transitions with participation of one of the higher-lying excited donor states $2p_-$, rather than of the lowest excited state $2p_0$ (fig. 6). Resonances, corresponding to $2p_0$–1s transitions, are much weaker, and the related series is revealed only as a result of the Fourier analysis of the curves dJ/dB (B^{-1}). Arrows in fig. 7 indicate energies of those donor excited states which have the longest lifetime. The lifetimes at $B = 0$ are 0.6, 0.3 and 0.4 ns for $2p_0$, 2s and $2p_-$ states, respectively (Gershenzon et al. 1979). The lifetimes of other excited states studied, are approximately an order of magnitude shorter. The fact that magnetoimpurity resonances observed in n-Ge take place for the transitions involving the most long-lived excited states (fig. 7), indicates that again we deal with center de-excitation in this material.

Thus, from two opposite resonance inelastic processes only one, the de-excitation of the center, was revealed in transport properties, practically in all cases when the option could be done.
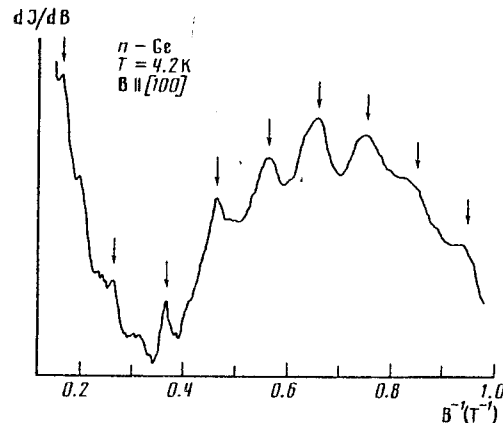

Fig. 6. The oscillations of the photoconductivity of n-Ge under infrared impurity photoexcitation. The periodical series of extrema, indicated by arrows, corresponds to the transition $2p_-$–1s (after Zverev and Shovkun 1984b).
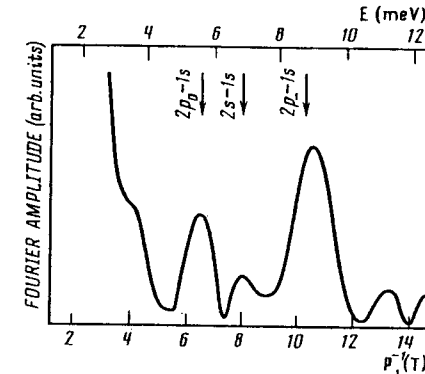
Fig. 7. The Fourier spectrum of the function dJ/dB (B^{-1}) from fig. 6. The energies, corresponding to transitions which involve the most long-lived excited donor states in Ge, are indicated by arrows.

3.2. Impact ionization and Auger recombination: n-InP

The transitions in which one of the states (initial or final) belongs to the lowest Landau level (the b–f transitions in fig. 2) is a special case of resonant inelastic electron–impurity scattering. By the accepted terminology these processes may be called resonant impact ionization if a carrier transition from the impurity state to the subband occurs, and resonant Auger recombination if a reverse process takes place.

Such processes have been observed by Eaves et al. (1974) and Nicholas and Stradling (1978). Figure 8 demonstrates resonance in the non-ohmic longitudinal magnetoresistance of n-InP. Extrema X_1, X_2 and X_3 satisfy the resonance condition (5) with ΔE equal to the ionization energy E_{ion} of a shallow donor. The most intensive is the extremum X_1, corresponding to $N = 1$ in eq. (5). As seen from fig. 9, this extremum is split. Analogous splitting was observed in the infrared photoconductivity response of the same sample. It is explained by the presence of two types of donors in the sample with different ionization energies. Thus, fig. 9 demonstrates the possibility of utilizing the magnetoimpurity resonances for studying shallow impurity spectra.

It is not yet clear, whether the magnetoimpurity process in n-InP involves heating or cooling of the free carriers. As follows from the measurements of the hot electron coefficient β [see eq. (9)], in moderate electric fields the first ($N = 1$) extremum of the curve $\beta(B)$ is a deep minimum, while the others are maxima (fig. 10). The interpretation of the measurements of the coefficient β is based on the electron temperature approximation. If this approximation is valid for n-InP, then in resonances corresponding to $N \geqslant 2$ resonant heating of electrons through the Auger recombination process occurs while for the fundamental ($N = 1$) peak resonant electron cooling through the impact ionization process
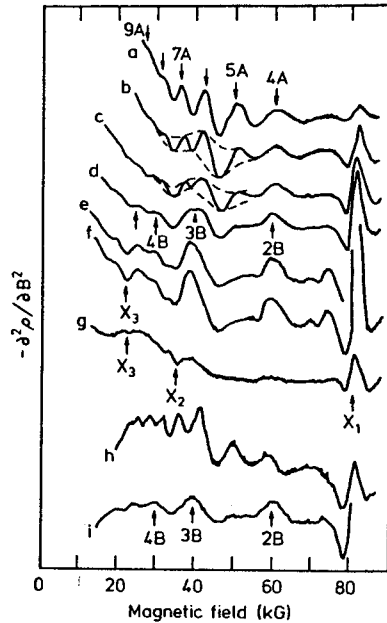
Fig. 8. Magnetoimpurity resonances in non-ohmic magnetoresistance of n-InP at 11 K. The peaks X_1, X_2 and X_3 are due to inelastic scattering, series A is the resonant capture of an electron by a donor assisted by LO-phonon emission, series B is the magnetophonon resonance (curves a to g are longitudinal, h and i transverse magnetoresistance) (after Eaves et al. 1974).
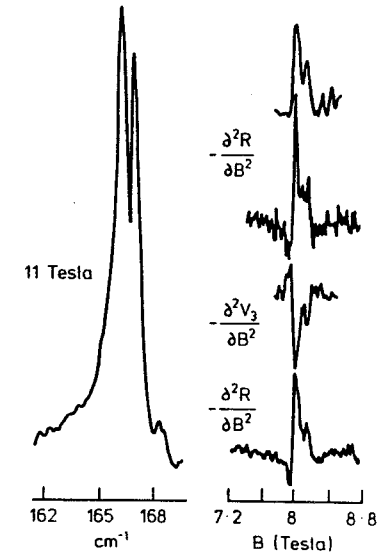

Fig. 9. Central cell structure in the $N = 1$ peak of the magnetoimpurity resonance at 20 K (on the right) and in the infrared photoconductivity response at 4.2 K (on the left) in n-InP. The upper curves on the right and the left curve correspond to the same sample (after Nicholas and Stradling 1978).
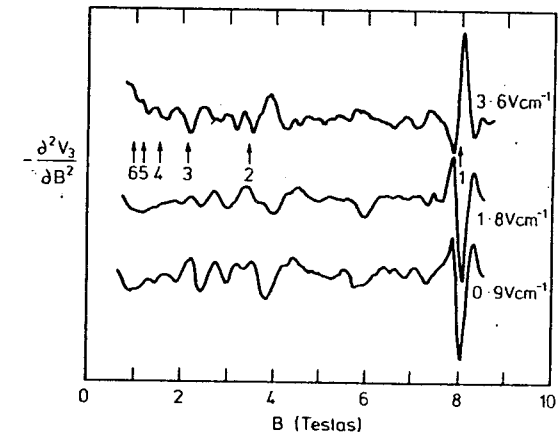
takes place instead. Evidently resonant scattering in this material deserves further investigation.

3.3. Decay of excitons at ionized impurities: p-Ge

Under interband photoexcitation a process of exciton decay at an ionized impurity accompanied by the impurity neutralization and a free carrier emission into the band can take place. In a p-type sample the hole transfers into the ground acceptor state, and the electron transfers into the conduction band. The energy conservation law for this process takes the form

$$- E_{ion}^{ex}(B) = n\hbar\Omega + \hbar^2 k_{\parallel}^2/2m_{\parallel} - E_{ion}^{a}(B), \qquad n = 0, 1, 2, \ldots . \tag{10}$$

At resonance $k_{\parallel} = 0$ and

$$\hbar\Omega(n + \tfrac{1}{2}) = E_{ion}^{a}(0) - E_{ion}^{ex}(0) + \delta(B). \tag{11}$$

Here the addition $\delta(B)$ is conditioned by the difference in the Zeeman and

Fig. 10. Magnetoimpurity resonances in the hot electron coefficient β in n-InP, registered by measuring the third harmonic component V_3 of the alternative voltage appearing down the sample in the constant-current mode (after Nicholas and Stradling 1978).

diamagnetic shifts of the ground state of the acceptor and exciton:

$$\delta(B) = \delta_a(B) - \delta_{ex}(B).$$

The term $\frac{1}{2}$ in the left part of eq. (11) arose from the contribution of the shift of the conduction band edge into the dependence E_{ion}^{ex} on B. The shift of the valence band edge does not enter eq. (11), since it enters both $E_{ion}^a(B)$ and $E_{ion}^{ex}(B)$.

For the first time the resonance process (11) was proposed by Rashba; it was considered by Zverev (1977) and Gantmakher et al. (1978) with reference to magnetoimpurity resonances in p-Ge. Figures 11 and 12 demonstrate this effect, observed under conditions of interband photoexcitation (Gantmakher and Zverev 1975, 1976a). As usual, the resonance manifests itself in oscillations of the photoconductivity. It is more convenient, however, to measure the electric field $\mathcal{E}$ of the photo-emf (see Kikoin and Lasarev 1967). Note the relative amplitude of the oscillations observed, which is of the order of unity in the range of small numbers. The oscillations are periodic in reciprocal field, the period depending on the chemical nature of the impurity (fig. 12). When the magnetic field deviates from the [100] axis, the extrema split, the multiplicity and the magnitude of the splitting corresponding exactly to the anisotropy of the electron cyclotron mass in Ge. Substituting experimental values of the periods and the electron cyclotron mass $m_c = 0.135 m_0$ in eq. (6), we obtain the following ΔE values:

$$\Delta E^{In} = 7.5 \text{ meV}, \quad \Delta E^{Ga} = 6.85 \text{ meV}, \quad \Delta E^B = 6.25 \text{ meV}.$$

These energies coincide within the limits of the experimental accuracy with the lowest excitation potentials of corresponding acceptors in Ge known from the spectroscopic measurements. This allowed us to ascribe this effect to resonances of inelastic electron scattering by acceptors (Gantmakher and Zverev 1975,
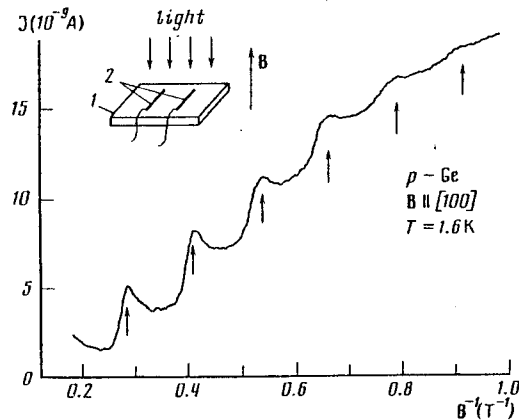

Fig. 11. The oscillations of the photoconductivity of p-Ge. Interband photoexcitation, the generation rate $G = 5 \times 10^{14}$ cm^{-3} (after Gantmakher and Zverev 1975).
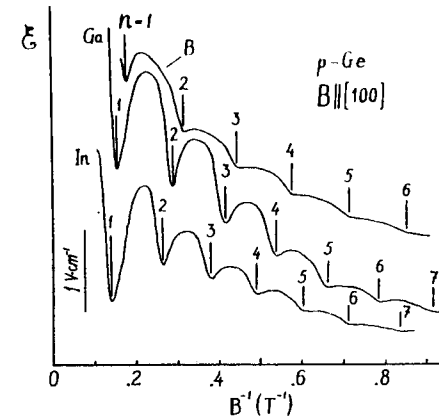
Fig. 12. The oscillations of the photoelectromagnetic emf $\mathcal{E}$ on the samples of p-Ge with different shallow acceptors. $T = 1.65$ K (after Gantmakher et al. 1978).

1976a). At the same time if we use the value $E_{ion}^{ex}(0) = 4.15$ meV for the binding energy of an indirect exciton in Ge (Altarelli and Lipari 1976) and experimental values of the ionization energy of acceptors (Haller and Hensen 1974) (for Ga in Ge $E_{ion} = 11.07$ meV), then for all shallow acceptors the value $\Delta E = E_{ion}^a(0) - E_{ion}^{ex}(0)$ would differ from the lowest potential of acceptor excitation only by 0.2 meV. The experimental ΔE values cited above prove to be lying just between the values of ΔE obtained from two different models: inelastic scattering and exciton decay.

Therefore, because of the accidental coincidence, it is not possible to distinguish the resonances (5) and (11) in p-Ge proceeding from their period only. To do this, further analysis is necessary based upon the dependence $\Delta E(B)$ as well as upon the results obtained in uniaxial stress experiments. Recent data on spectroscopy of shallow acceptors in Ge facilitate the task.

The splitting of the acceptor ground state in the magnetic field is very small (Tokumoto and Ishiguro 1977, Freeth et al. 1986). Therefore, to compare the magnetic field dependences of the energies ΔE for the two models under consideration one can neglect the $E_{ion}^a(B)$ dependence and take into account only the $E_{ion}^{ex}(B)$ and $E_{ion}^*(B)$ dependences ($E_{ion}^*(B)$ is ionization energy of the lowest acceptor excited state). Such comparison is shown in fig. 13. Experimental values of the resonant fields B_n determine energies $n\hbar\Omega_n$ marked on the fan of straight lines. The field dependence of the energy transferred to the electron according to the exciton decay model (solid curve) was obtained from magnetooptical measurements (Martin et al. 1976). Similar data about the value $E_{ion}^a(B) - E_{ion}^*(B)$ were available only in the fields $B \leqslant 2$ T (Soepangkat and Fisher 1973). However, in the higher field region the Zeeman splitting of the
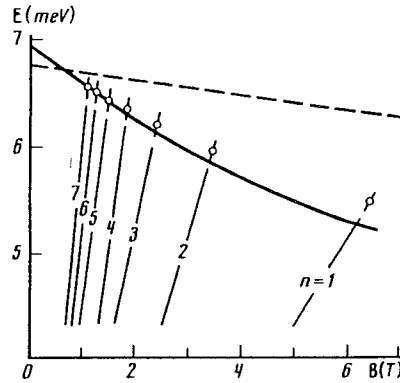
Fig. 13. The energy transfer in magnetoimpurity resonances in p-Ge. Circles are experimental values $n\hbar\Omega$, the solid curve is the exciton decay model, the dashed curve the inelastic scattering model (the positive diamagnetic shift is omitted).

lowest acceptor excited level can be deduced from the line splitting in the effect of resonant capture of light holes (see fig. 21 of this chapter). These data are in agreement with those obtained by Soepangkat and Fisher (1973) in the low field region. In fig. 13 the linear part of the $E_{ion}^a - E_{ion}^*$ dependence on B is shown by a dashed curve. If the diamagnetic shift of E_{ion}^* were taken into account (this shift is not known in the high field region), then experimental points should lie above the dashed curve in fig. 13.

Thus, the analysis of data presented in fig. 13 favours the exciton model, eq. (11). Besides, the splitting of magnetoimpurity resonances in stressed p-Ge (Zverev 1977) contradicts the inelastic scattering model. Figure 14 shows the effect of stress $F \parallel [100]$ on a Ga-doped sample with $B \parallel [001]$. In this configuration all the conduction band ellipsoids behave similarly. As seen from the figure, two series of extrema arise under deformation. The corresponding energies $\Delta_{1,2} E$ versus the stress are plotted in fig. 15. One of the components is practically independent of stress whilst the other shifts to lower energy. The energy difference $\Delta_1 E - \Delta_2 E$ coincides to an accuracy of about 10% with the value of splitting of the acceptor ground state known from spectroscopic data of Martin et al. (1983). It follows, however, from these very data that the deformational splitting of the lowest excited state of the acceptor at $F \parallel [100]$ is about 6 times smaller than the ground state splitting. This means that the component $\Delta_1 E$ in fig. 15, which is practically independent of F, cannot be ascribed to any transition between splitting levels of the ground and lowest excited states of the acceptor.

Thus, it turns out that under interband photoexcitation magnetoimpurity resonances in p-Ge are caused by exciton decay at an ionized acceptor.
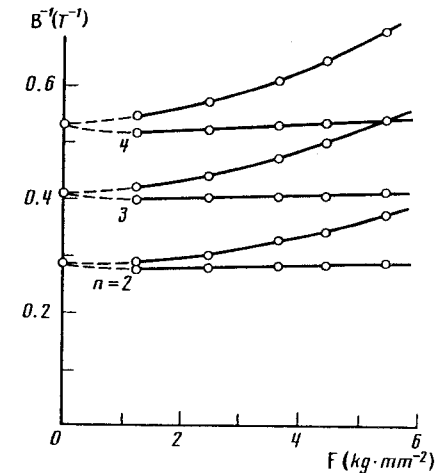
Fig. 14. Dependence of the magnetoimpurity resonance positions on the uniaxial stress in p-Ge. $F \parallel [100]$, $B \parallel [001]$.
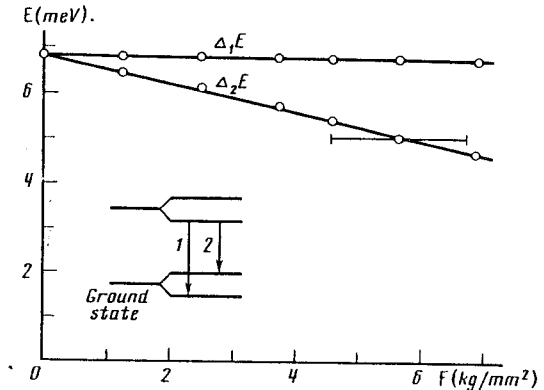

Fig. 15. Dependence on the uniaxial stress of the energies $\Delta_1 E(0)$ and $\Delta_2 E(0)$, see fig. 14.

3.4. Resonant photoionization

By resonant photoionization we mean the b–f transitions called forth by monochromatic excitation. By changing the field B or the photon energy $\hbar\omega$ one can force the absorption coefficient to oscillate, increasing sharply each time, when the final state approaches a Landau level. Usually the sample width is much less than the reciprocal of the light absorption coefficient. Hence, alongside with the absorption coefficient the total number of photocarriers and hence photoconductivity also oscillates.

Oscillations of magnetoabsorption provided by resonant photoionization of shallow Coulomb centers were firstly observed by Fisher and Fan (1959) on germanium samples doped by boron. Corresponding photoconductivity measurements were carried out on p-Ge (Kaplan et al. 1968, Zverev 1978, 1980), n-Ge (Zverev 1978), n-GaAs (Ivanov and Lifshits 1978, Zverev and Shovkun 1986). At first, the spectra were interpreted by assuming that photoionization transitions occur directly to the f-levels (Fisher and Fan 1959). However, further investigations revealed that photoionization occurs in two stages via qb-states by subsequent b–qb and qb–f transitions (fig. 2). The resonant condition for the b–qb processes has the form

$$\hbar\omega = E_{nj} - E_{0i}, \qquad n = 1, 2, \ldots . \tag{12}$$

Here $\hbar\omega$ is the photon energy, E_{nj}, E_{0i} are the energies of the qb- and b-states, indices j and i denote sets of quantum numbers m and μ, defining the corresponding states [see eq. (3)]. The fact that the energy E_{nj} of the qb-state rather than the energy E_n of the Landau level enters eq. (12), follows from the analysis of the resonant magnetic fields. In fig. 16 the photoconductivity of

n-GaAs, excited by a laser with the wavelength 78.4 µm is plotted as a function of B, and fig. 17 shows the fitting of this plot (Ivanov and Lifshits 1978). A fan of straight lines, coming out of the point $E = Ry^*$ shows the spectrum of Landau levels in the conduction band. The experimental points, including those which correspond to the main series of resonances do not fit the straight lines. Since the spectrum of electrons as well as the shallow donor spectrum in GaAs is known, it is possible to determine the qb-levels to which transitions occur. According to Ivanov and Lifshits (1978), the main series of resonances corresponds to transitions allowed by selection rules from the ground state (000) to Coulomb states with indices (n10).

In analyzing the experiments on GaAs (figs. 16 and 17) the electron dispersion law was supposed to be parabolic. This was possible since the photon energy was small and electrons were excited rather close to the bottom of the band. Often, however, the nonparabolicity of the dispersion law becomes important. Then, instead of eq. (1), it is necessary to use the quasiclassical condition of quantization of the carrier orbit area $S(E)$ in k-space:

$$S(E_n) = 2\pi e B(n + \gamma)/c\hbar, \qquad |\gamma| < 1. \tag{13}$$

In a parabolic band the function $S(E)$ is linear. The value E_{nj} is fixed by the resonance condition (12). It can be written as

$$E_{nj} = E_n + \varepsilon_{nj} \pm \tfrac{1}{2}\mu_B g B, \tag{14}$$

where, in comparison with eq. (3), the spin splitting of the Landau levels is taken into account ($\varepsilon_{nj} < 0$ is the Coulomb energy, $\mu_B = e\hbar/2m_0 c$ is the Bohr magneton,
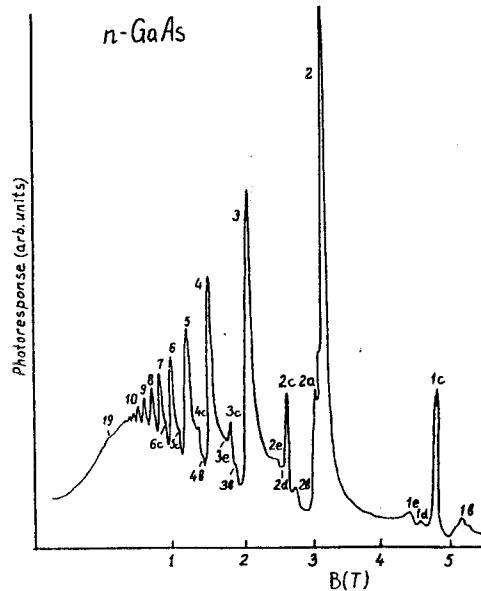

Fig. 16. The spectrum of photoconductivity of n-GaAs under the far-infrared laser excitation. The wavelength 78.4 µm, $T = 4.2$ K. The magnetic field scale is nonlinear (after Ivanov and Lifshits 1978).
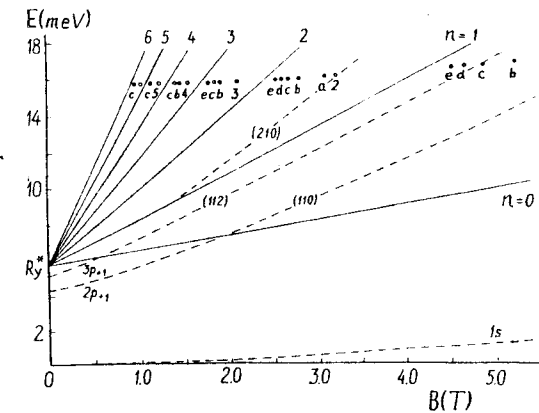

Fig. 17. Fitting of the experimental data obtained from the resonance photoionization spectrum (fig. 16) to the spectrum of quasibound and free states of an electron in n-GaAs in a magnetic field (after Ivanov and Lifshits 1978).

g is the effective g-factor). Expanding $S(E)$ into a series near E_{nj}:

$$S(E_{nj}) = S(E_n) + \partial S/\partial E(\pm \tfrac{1}{2}\mu_B gB + \varepsilon_{nj})$$

and using eq. (13), we get after simple transformations

$$B_n^{-1} = \frac{2\pi e}{chS}(n + \gamma \pm gm_c/4m_0 + \varepsilon_{nj}/\hbar\Omega_n). \tag{15}$$

Here we have used the definition of the cyclotron mass

$$m_c = (\hbar^2/2\pi)\,\partial S/\partial E.$$

It follows from eq. (15) that resonant field values are periodic in reciprocal field with the period

$$P = 2\pi e/chS, \tag{16}$$

determined by the area of the extremal cross section of the constant-energy surface $E = \hbar\omega - |E_{0i}|$ in k-space by a plane perpendicular to magnetic field. Deviations from the periodicity are governed by the field dependence of the ratio $\varepsilon_{nj}/\hbar\Omega_n$ for a fixed energy in the band. If the dependence is weak, the Coulomb energy, as seen from eq. (15), leads only to a phase shift of oscillations and does not affect their periodicity.

Nonparabolicity of the spectrum is important, for example, in p-Ge when the resonant photoionization of acceptors into the light hole band leads to photocurrent oscillations. These oscillations at different wavelengths of monochromatic excitation are presented in fig. 18. They are periodic in reciprocal field to a great accuracy. The period measured at different values of

the exciting photon energies allows to find the functions $S(E)$ and $m_c(E)$. The latter is shown in fig. 19. The extrema splitting caused by the spin splitting of the Landau levels of the light hole gives information on the effective g-factor of light holes in Ge and its energy dependence (Gantmakher et al. 1983).

Note that all the information about the light hole spectrum in Ge is obtained only from the oscillation periods. To find the Coulomb energy $\varepsilon_{nm\mu}$ [see eq. (3)] this, however, is not sufficient. This energy is determined by a small difference ΔB between two large field values: the first, making the transitions to qb-states resonant, and the second, satisfying eq. (12) with E_n instead of E_{nj}. The first is measured in the experiment, the second must be calculated. Due to the valence band degeneracy in Ge, these calculations are to be done numerically. The Coulomb energy thus obtained can be compared with the theoretically calculated one. The realization of such a program for p-Ge by Gantmakher et al. (1983) showed a good agreement with the theory of both the spectra of Landau levels in valence band and binding Coulomb energy in the magnetic field. The comparison was made, supposing that actually stationary states with quantum numbers $(nn0)$ are involved in the transitions. However, it follows from fig. 2 of the paper by Gantmakher et al. (1983) that the energy difference between these levels and the $(n10)$ levels distinguished by selection rules for optical transitions does not exceed the experimental error.

Note in conclusion that not only shallow hydrogen-like impurities can be ionized resonantly in a magnetic field, but also centers of other origin, e.g., $D^-(A^+)$-centers formed by electron (hole) bounded to a neutral donor (acceptor). For the first time, such resonances in photoconductivity were observed under the photoionization of D^--centers in Ge doped with antimony and arsenic (Tanigushi and Narita 1979), and then of D^--centers in Si (Narita
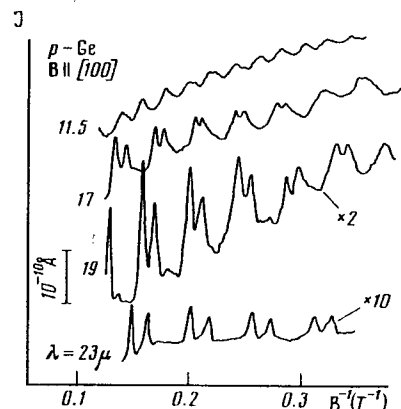
Fig. 18. The oscillations of the photocurrent in p-Ge at different wavelengths of infrared illumination. The wavelength is indicated near the curves. $T = 1.6$ K (after Zverev 1980).
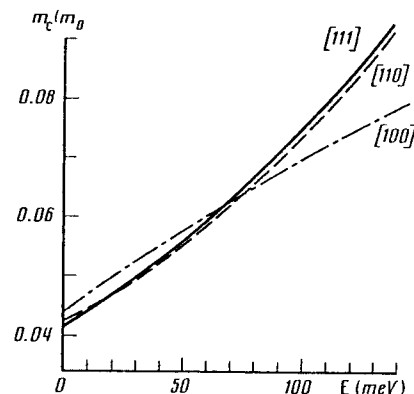
Fig. 19. The energy dependence of the cyclotron mass of light holes in Ge at different directions of the magnetic field, measured in the resonant photoionization experiments (after Zverev 1980).

1984, 1985) and A^+-centers in Ge (Nakata et al. 1986). However the resolution achieved in these experiments was not sufficient to discriminate transitions to f-levels and qb-levels.

3.5. Resonant capture with phonon emission

The process opposite to photoionization is carrier capture from the vicinity of the magnetic subband bottom to one of the b-states of the impurity center accompanied by emission of a quasiparticle with energy $\hbar\omega$. For resonance to occur, some specific energy $\hbar\omega$ should be singled out from other energies. It may be, for example, the energy of an optical phonon. The corresponding resonant process is described by the same eq. (12): a carrier hits first a qb-level E_{nj} in the vicinity of the impurity center, and next transits to a level E_{01} emitting an optical phonon. The energy $\hbar\omega$ in this process equals the optical phonon energy $\hbar\omega_0$.

This resonant process of carrier capture by impurities often accompanies the usual magnetophonon resonance. Owing to the factor $\exp(-\hbar\omega_0/kT)$, appearing in the expression for the amplitude of the magnetophonon resonance, it can be observed only at $T \gtrsim 40$ K. At lower temperatures the mobility is limited by electron scattering by acoustic phonons and impurities. However, under non-ohmic conditions, when the electron temperature becomes even slightly higher than the lattice temperature, oscillations arise. For several semiconductors their period, though being close to the period of magnetophonon oscillations, differs from the latter. This is just the resonant capture by impurities. Such oscillations were first observed in non-ohmic magnetoresistance of n-InSb at 4 K by Kotera et al. (1966), and then in other materials both under non-ohmic conditions (see, e.g., the review by Harper et al. 1973) and under the photoexcitation (Parfen'ev et al. 1967, Instone et al. 1977, Gantmakher and Zverev 1980). In fig. 3 these oscillations in n-GaAs are seen along with inelastic scattering resonances. Figure 20 shows how the resonant capture is gradually replaced by the usual magnetophonon resonance, as temperature is increased.

The results of most experiments on resonant capture were interpreted in terms of transitions directly from the Landau levels (Harper et al. 1973). Then the experiments on p-Ge, where the resonance lines happened to be very narrow, permitted one to prove experimentally that qb-states are an intermediate stage in the capture process (Gantmakher and Zverev 1980).

In some cases it is possible to observe carrier capture both into the ground and excited b-states of the impurity. Figure 21 demonstrates a fragment of the spectrum with resonance lines corresponding to transitions from qb-states below magnetic subbands of light holes 2_2 and 3_1 to the ground and to four excited b-states of the acceptor in p-Ge.

Resonant capture experiments yield information analogous to that obtained from studies of resonant photoionization, with the resolution comparable to that obtained with laser photoexcitation. For instance, the splitting of those lines in fig. 21 which corresponds to transitions into excited acceptor states is
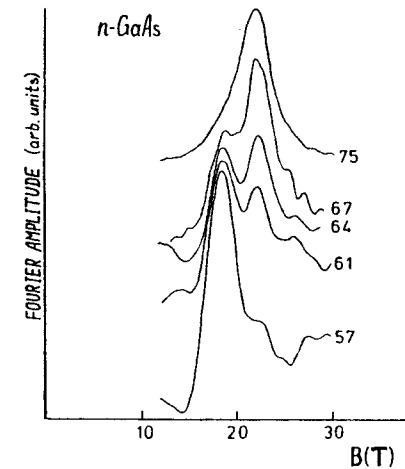
Fig. 20. Fourier spectra of the magnetophonon oscillations in n-GaAs at different temperatures (indicated in Kelvin for each curve) (after Nicholas and Stradling 1976).
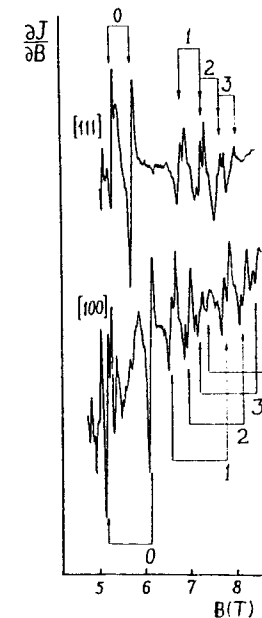

Fig. 21. Resonance capture of light holes from qb-states below the Landau levels 2_2 and 3_1 to the ground (0) and four excited (1–4) states of acceptors in Ge. The field B direction is indicated near the curves. $T = 1.6$ K (after Gantmakher and Zverev 1980).

caused by the Zeeman splitting of these states. Such splitting can be easily measured. Note that Zeeman splitting of the ground state is very small (Tokumoto and Ishiguro 1977), so the corresponding lines in fig. 21 are not split.

3.6. Resonances in magnetoresistance of p-Te

Non-ohmic magnetoresistance of p-Te doped with elements of the V group (Bi, Sb, As, P) exhibits two types of resonances (von Klitzing 1978). The first one is a series of extrema, periodic in reciprocal field and caused by magnetoimpurity resonances of inelastic scattering. Apart from them, single resonance lines were observed, their position also depending on the chemical nature of the impurities (figs. 22, 23). To elucidate the origin of these resonances, von Klitzing and Tuchendler (1981) carried out a study of the acceptor energy spectrum in Te in a magnetic field by means of infrared spectroscopy techniques. Due to the 'camel's back' shape of the valence band edge the ground state of a shallow acceptor in Te is split into two states with symmetric and antisymmetric wave functions (bonding and antibonding states). The splitting depends on the magnetic field growing with an increase of B (fig. 24). Von Klitzing and Tuchendler (1981) found that at the resonance fields the valley-orbital splitting of the ground state equals half the excitation potential of the acceptor $2p_-$-state, i.e., the antibonding level occurs to be in the middle between the bonding and the $2p_-$-levels.

Denoting the bonding, antibonding and $2p_-$-states of the hole by $|0\rangle$, $|1\rangle$ and $|2\rangle$, and the energy difference between $|i\rangle$ and $|j\rangle$ levels by E_{ij} $(i, j = 0, 1, 2)$, we can write the experimentally obtained resonance condition in the form
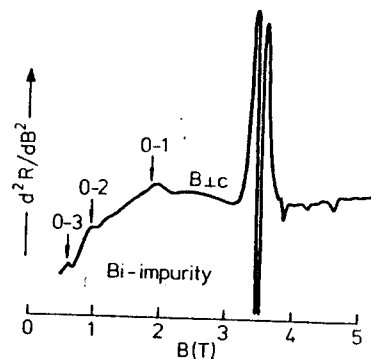
$$E_{10} = E_{21}. \tag{17}$$

Fig. 22. Resonances in non-ohmic magnetoresistance of p-Te. The arrows indicate the resonant fields calculated for the first three numbers of resonances in inelastic scattering with the energy transfer corresponding to the lowest excitation potential of the acceptor (after von Klitzing 1978).
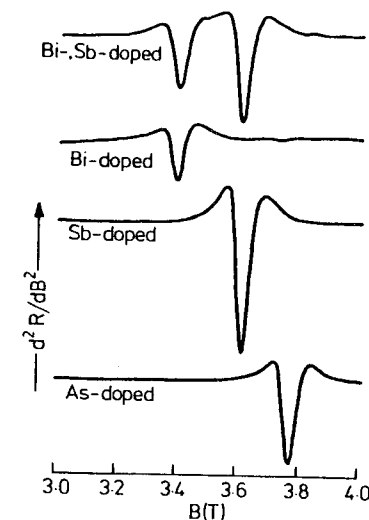
Fig. 23. The influence of the chemical nature of impurities in Te on the line position of the magnetoimpurity resonance in the high field region (after von Klitzing 1978).

Equation (17) is rather specific. It contains only gaps from the impurity spectrum and does not contain energies of free carriers. Gantmakher and Levinson (1986) proposed an explanation of the phenomenon based on the analysis of the two-phonon de-excitation transitions $|2\rangle \rightarrow |0\rangle$.

The interaction between an impurity electron and the lattice vibrations has the form $V = V_1 + V_2$, where V_1 is the one-phonon interaction and V_2 is the two-phonon interaction. The transition $|2\rangle \rightarrow |0\rangle$ accompanied by emission of two phonons q and q' appears in the second order of perturbation theory in V_1 and in the first order in V_2, therefore the corresponding matrix element has the form

$$M_{qq'} = M_{qq'}^{(1)} + M_{qq'}^{(2)},$$

where

$$M_{qq'}^{(1)} = \langle 2|V_2|0; q, q'\rangle,$$

$$M_{qq'}^{(2)} = \frac{\langle 0; q, q'|V_1|1; q\rangle \langle 1; q|V_1|2\rangle}{E_{21} - \hbar s q + i\hbar/\tau_1} + \dots. \tag{18}$$

Here the dots mean a term obtained from that written above by permutation of q and q'; $\hbar s q$ is the phonon energy (s is the sound velocity), τ_1 is the lifetime of the state $|1\rangle$, $|\alpha; q, q', \dots\rangle$ denotes a state of the 'impurity + lattice' system when phonons $q, q', \dots$ are excited.
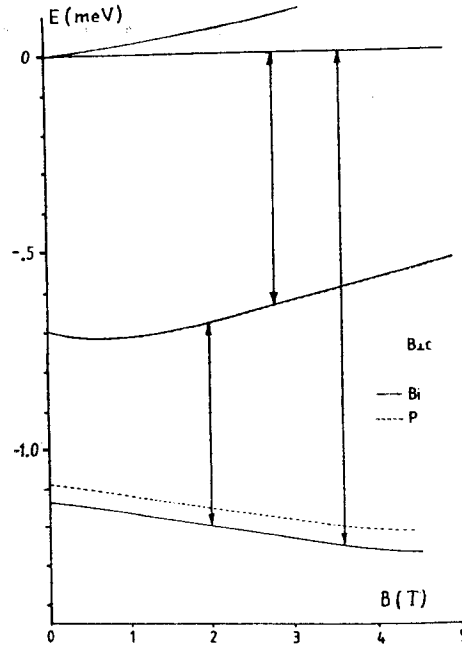
Fig. 24. Energy level scheme of shallow acceptors Bi and P in Te. The energy is measured with respect to the level of 2p_-state (after von Klitzing and Tuchendler 1981).

The probability of the transition in question is

$$W_{qq'} = \frac{2\pi}{\hbar} |M_{qq'}|^2 \delta(E_{20} - \hbar s q - \hbar s q').$$

The matrix element $M^{(1)}$ contains an integral

$$\int d^3 r \, \psi_2^*(r) \, \psi_0(r) \, \exp[i(q + q')r]. \qquad (19)$$

Therefore, it is not small only if $|q + q'|a \lesssim 1$, i.e., when

$$|q| \approx |q'| \approx E_{20}/2\hbar s. \qquad (20)$$

The matrix element $M^{(2)}$ is large for such phonons, the denominator in (18) is small, i.e., when

$$\hbar s q \approx E_{21}, \qquad \hbar s q' \approx E_{10}, \qquad (21)$$

i.e., when the two-phonon transition $|2\rangle \to |0\rangle$ through a virtual intermediate state 'reduces' to a sequence of two one-phonon transitions through a real intermediate state. The square $|M_{qq'}|^2$, entering the transition probability, contains an interference term $M_{qq'}^{(1)} \cdot M_{qq'}^{(2)*} + $ c.c., large only when both con-

ditions (20) and (21) are satisfied, i.e., when $E_{21} = E_{10} = E_{20}/2$. It seems that this very term accounts for resonances demonstrated in fig. 23.

The relation (20) is satisfied to an accuracy of $\Delta q \approx 1/a$, and the relation (21) to an accuracy of $\Delta q \approx 1/\tau_1 s$. Therefore the width of the interference resonance on the energy scale, i.e., the allowed deviation of the level $|1\rangle$ from the middle of the gap E_{20} is

$$\delta E \approx \hbar s/a + \hbar/\tau_1. \qquad (22)$$

Estimating energy δE from eq. (22) (it appeared to be approximately 0.2 meV) one can determine with the help of fig. 24 the width of the resonance line in the field scale. This estimate satisfactorily agrees with the experiment.

If the explanation suggested is correct, the resonance in Te is, strictly speaking, beyond the scope of this chapter, since free carriers do not take part in this resonance. However, it resembles much the resonance in inelastic scattering in its experimental manifestations and conditions of its observation. As seen from fig. 22, the long-lived impurity state decays more efficiently via the interference resonance than via inelastic scattering resonances.

3.7. Magnetoimpurity resonances in elastic scattering

To make the classification complete, we mention two resonances in elastic scattering of free carriers by impurities in quantizing magnetic fields.

One of them was predicted by Gurevich (1967) for many-valley semiconductors with valleys shifted in energy. The probability of elastic inter-valley transitions has a maximum, if the following condition is valid:

$$\hbar\Omega_\alpha(n_\alpha + \tfrac{1}{2}) + \Delta E_{\alpha\beta} = \hbar\Omega_\beta(n_\beta + \tfrac{1}{2}). \qquad (23)$$

Here the indices α and β correspond to two different valleys shifted with respect to each other by the energy $\Delta E_{\alpha\beta}$ (see fig. 25). For an elastic transition to occur, it is necessary for the occupation number of the final state to differ from unity. This means that under equilibrium conditions we deal either with Boltzmann statistics, or, in the case of Fermi statistics, with resonances in a layer kT near
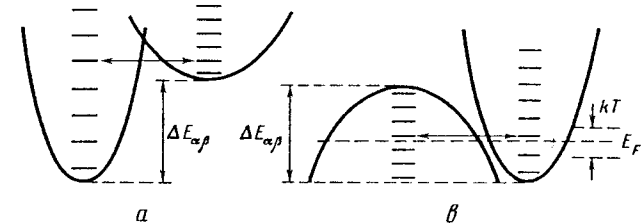

Fig. 25. The resonant transitions in a magnetic field for the elastic electron scattering by impurities: (a) semiconductor with shifted valleys, (b) semimetal.

the Fermi energy E_F. In the latter case the field and the temperature should satisfy inequalities

$$h/\tau \ll \hbar\Omega \ll kT \ll E_F.$$

Shifted valleys exist in semiconductors of the n-GaAs type. They can be also obtained by applying the uniaxial stress in the many-valley semiconductors, such as Ge and Si. As a third example, semimetals may be mentioned, where energy bands overlap. In the last case Ω_α and Ω_β in eq. (23) have opposite signs.

The increase of the scattering probability in resonances should alter the DC conductivity and other transport properties of the sample thus leading to oscillations with changing B. In general, the picture of oscillations should be rather complicated, especially if the Landau levels are spin-split. The most simple case is when $\Omega_\alpha = \Omega_\beta$. This equality holds, for example, in stressed n-Ge at $B \parallel [100]$ or n-Si at $B \parallel [111]$. In this case the probability of inter-valley transitions will oscillate periodically in the reciprocal field with the period (6) determined by the energy $\Delta E_{\alpha\beta}$.

Up to now, resonances (23) have not been observed. However, there exist an unexplained experiment in Bi (Bogod et al. 1980) in which oscillations of unknown nature were observed, with maximal amplitude near 10 K.

One more type of resonances, also unobserved up till now, is related to the scattering of low energy carriers in the field of an attracting center. The scattering cross section increases when one of the discrete impurity levels happens to be located close to the bottom of the band (Landau and Lifshits 1977). By changing the magnetic field one can affect the electron spectrum of the center and push the discrete levels out of the well one by one. When any of these levels approaches the continuous spectrum, the probability of elastic scattering is expected to increase. Andreev (1979) paid attention to this effect and showed that it can be realized in semiconductors with an anisotropic electron spectrum $(m_1 = m_2 = m_\perp \ll m_\parallel = m_3)$, containing short-range attracting centers of radius a smaller than the magnetic length $\lambda = (c\hbar/eB)^{1/2}$. If the magnetic field is directed along the longitudinal axes of the constant-energy ellipsoid, then, for the effect to take place, the condition

$$\hbar^2/m_\parallel a^2 \ll |U(0)| \ll \hbar^2/m_\perp a^2 \qquad (24)$$

should be satisfied. Here $U(z) < 0$ is the effective one-dimensional potential for electron motion along B.

The potential $U(z)$ is obtained by averaging the spherically symmetric field $V(r)$ with the finite radius a over wave functions of the free states in the plane, perpendicular to B. The right part of the inequality (24) provides nonmixing of magnetic subbands and allows one to reduce the problem to scattering in a one-dimensional magnetic subband. The left inequality provides the existence of several bound states in the one-dimensional well $U(z)$. If the field B is decreasing, the well depth diminishes and levels get out of the well giving rise to oscillations

of the scattering probability and the conductivity. If the screened Coulomb potential

$$V(r) = -(\alpha/r)\exp(-r/a), \qquad \alpha > 0$$

is taken as the initial one, the oscillations appear to be periodic with the square root of the magnetic field.

4. Influence of resonances on the transport coefficients

It is rather simple to trace the influence of resonant photoionization or capture on transport coefficients. We know qualitatively how the numbers of carriers and ionized centers change at resonance. The arising complications are of experimental, methodical character. Consider, as an example, changes in the lineshape observed by Kaplan et al. (1968) in resonant photoionization spectra of p-Ge. In these experiments photocurrent maxima changed into minima when either the sample width, or the impurity concentration increased. The effect was brought about by changes in the relation between the sample width d and the inverse coefficient α^{-1} of the light absorption. At $d \ll \alpha^{-1}$ there is always a maximum at resonance, whereas at $d \gg \alpha^{-1}$ the form of the resonance extremum is determined by competing contributions of resonantly excited carriers and of those moulding the background signal.

The case of inelastic scattering of free carriers or excitons by impurities is more complicated. One needs to explain, for example, why and how resonant decay of excitons at ionized centers can change photoconductivity of p-Ge by a factor of two (fig. 11). In such a process not only free electrons are excited but also the concentrations of excitons and ionized impurities change. The problem is that we have to deal with a multicomponent system, in which the equilibrium is shifted by resonance.

The simplest system of excitations takes place when all the carriers have the same sign. Such a system can be realized either by means of impurity excitation or by applying electric fields large enough to reach the non-ohmic regime at low temperatures. We consider below inelastic scattering at photoexcitation, regarding de-excitation of centers as dominant resonant process.

4.1. Three-level model

Let us analyze how the inelastic electron scattering by excited impurities affects the conductivity. In what follows, we assume a material with shallow donors, but everything is applicable to acceptors also. Consider a three-level model (fig. 26) in which the upper level (f) corresponds to free electrons, and the middle (1) and the lowest (0) to excited and ground donor states, respectively. We can describe all free states by means of one level, based on the very strong temperature dependence of both magnetoimpurity resonances and the background
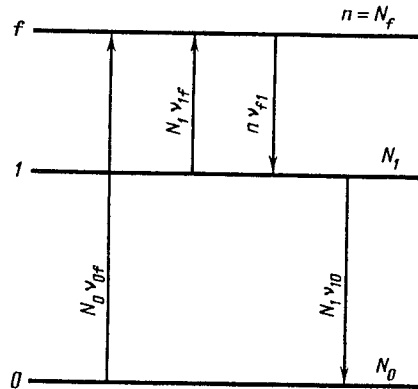
Fig. 26. Transitions in a three-level system, eq. (25).

photoconductivity (Zverev and Shovkun 1984a, b). The energies of the electrons excited by the room temperature infrared radiation in these experiments are of the order of a dozen meV. But, as their lifetime is much larger than the energy relaxation time, most of the electrons have energy $E \approx kT \ll \hbar\Omega$, i.e., they are in the lowest Landau level. By the excited level in the model we mean one or several of the most long-lived excited donor states. According to the previous section, the most long-lived is, as a rule, the lowest excited impurity state.

The concentration n of free electrons, as well as populations N_1 and N_0 of the excited and the ground donor states are related by the following set of equations:

$$nv_{f1} = N_1 v_{1f} + N_0 v_{0f},$$

$$N_1(v_{10}^{ph} + v_{10}^e + v_{1f}) = nv_{f1},$$

$$N_0 + N_1 + n = N_d - N_a. \tag{25}$$

Here v_{ij} is the probability of electron transition $i \to j$ from level i to level j (i, $j = 0, 1, f$), the probability of transition $1 \to 0$ is divided in two parts v_{10}^{ph} and v_{10}^e related to spontaneous phonon emission and inelastic scattering, respectively, N_d and N_a are the donor and acceptor concentrations. We introduce also the probability of inelastic electron scattering W_{ie} related to the scattering cross section σ_{10} by usual formula

$$W_{ie} = N_1 \bar{v}\sigma_{10},$$

where $\bar{v}$ is the electron velocity. Similarly, $v_{10}^e = n\bar{v}\sigma_{10}$. The probabilities W_{ie} and v_{10}^e are related by the evident relationship

$$nW_{ie} = N_1 v_{10}^e. \tag{26}$$

Using the second equation of the system (25) and eq. (26) we get

$$W_{ie} = v_{f1} \frac{v_{10}^e}{v_{10}^e + v_{10}^{ph} + v_{1f}}. \tag{27}$$

In the further analysis of eq. (27) we shall assume that infrared illumination makes $v_{1f} \ll v_{10}^{ph}$ even for long-lived excited donors. For GaAs it was proved experimentally by Zverev and Shovkun (1984a).

4.2. Limiting cases: n-Ge and n-GaAs

Consider two important limiting cases. If the inequality

$$v_0^{ph} \gg v_{10}^e \tag{28}$$

holds, the probability v_{10}^e does not enter eq. (25). Therefore at resonance, as seen from eq. (27), W_{ie} grows with increasing v_{10}^e, while the concentration N_1 does not change.

According to estimates for donors in Ge, the time $\tau^{ph} \equiv (v_{10}^{ph})^{-1}$ is small and the relation (28) is satisfied with a great reserve (Zverev and Shovkun 1984b). This means that magnetoimpurity oscillations of conductivity in n-Ge are due to W_{ie} oscillations. In this case the amplitudes of series, corresponding to different excited donor states, should be proportional both to their lifetime and to changes, due to the resonance, in corresponding cross sections of inelastic electron scattering:

$$\delta W_{ie} = N_1 \bar{v}\delta\sigma_{10} \propto \tau^{ph}\delta\sigma_{10}. \tag{29}$$

Which of these factors turns to be more important, depends on specific parameters. As found by Gershenzon et al. (1979), in n-Ge the lifetimes of most long-lived excited states ($2p_0$, 2s and $2p_\pm$) are 0.6, 0.3 and 0.4 ns, respectively. However, the donor in the $2p_0$-state has a cross section of about an order of magnitude less than in the $2p_-$-state, since the binding energy of the $2p_0$-state is greater. This explains why in the Fourier spectrum of magnetoimpurity resonances in n-Ge (fig. 7) the lowest excited state $2p_0$ produces a smaller amplitude than the $2p_-$-state. For the same reason and, in addition, due to a still less lifetime, the participation of the 2s-state in resonant scattering should be even smaller.

Each inelastic scattering event is followed by a cascade process of acoustic phonons emission by the carrier. In a formal way it can be accounted for by introducing a coefficient $r \gg 1$ into the relation

$$(\tau_p)^{-1} = v_0 + rW_{ie},$$

where τ_p is the momentum relaxation time, v_0 is the probability of carrier scattering via all other channels: elastic, phonon, etc. This coefficient indicates that even at a relatively small frequency of inelastic scattering ($W_{ie} \ll v_0$) its contribution to mobility can be large.

In the other limit

$$v_{10}^{ph} \ll v_{10}^{e} \tag{30}$$

it is the number N_1 that changes at resonance, since as it follows from the second equation of the system (25), $N_1 = nv_{f1}/v_{10}^e = v_{f1}/\bar{v}\sigma_{10}$. At the same time, the probability W_{ie} does not change, since the growth of the cross section σ_{10} at resonance is compensated by decreasing N_1. The conductivity alters in this case because a variation in the number N_1 of excited impurities shifts the equilibrium in the system and changes the number n of free carriers. This limiting case is realized in n-GaAs (Zverev and Shovkun 1984a). Besides numerical estimates, this follows also from comparison of the longitudinal ($J \parallel B$) and transverse ($J \perp B$) photoconductivities: in both cases magnetoimpurity resonances have the form of minima. Therefore one can conclude that it is not the mobility of photoelectrons that oscillates, but their concentration.

To elucidate the relation between changes in N_1 and n, we solve the system (25) with respect to the concentration of nonequilibrium carriers

$$n = (N_d - N_a)(v_{0f}/v_{f1})$$

$$\times \frac{1 + v_{1f}/v_{10}^e}{1 + (v_{0f}/v_{f1})(1 + v_{f1}/v_{10}^e + v_{1f}/v_{10}^e)}. \tag{31}$$

In n-GaAs the probabilities v_{0f} and v_{1f} are small as compared to the probabilities v_{f1} and v_{10}^e. Under these conditions, the change in $\tau^e \equiv (v_{10}^e)^{-1}$ at resonance leads to a relative change in the free carrier concentration, equal to

$$\delta n/n = (v_{1f} - v_{0f})\delta\tau^e. \tag{32}$$

In contrast to eq. (29), the value $\delta\tau$ enters eq. (32) rather than δv. At $v_{1f} = v_{0f}$ redistribution of the population of the ground and excited states at resonance does not alter the overall generation rate, therefore $\delta n = 0$. If $v_{1f} \neq v_{0f}$, the sign of the effect depends on which of two considered bound states has larger ionization probability.

Thus, even in a simple three-level model both the increase and the decrease in the concentration of free electrons can occur at resonance depending on relations between specific parameters of the material.

In the experiments we are discussing here, the donors are ionized mainly by hot electrons. Each photoexcited electron can ionize several donors, so that v_{1f} and v_{0f} are determined by impact ionization. Believing that the impact ionization cross section σ_{if} for an impurity center is close to its geometric cross section (Palmier 1972), we get $v_{1f}/v_{0f} \cong \sigma_{1f}/\sigma_{0f} \cong 10$.

Thus, instead of eq. (32), we can write

$$\delta n/n = v_{1f}\delta\tau^e. \tag{33}$$

The relation (33) gives the correct sign of the variation of the carrier

concentration at resonance, i.e., $\delta n < 0$ when τ^e decreases. It also allows one to explain, why in the concentration range studied ($5 \times 10^7 \text{ cm}^{-3} < n < 5 \times 10^8 \text{ cm}^{-3}$) the amplitude of magnetoimpurity resonances is independent of the generation rate. Since at resonance the τ^e variation can be large [Pidgeon et al. (1983) stated that in the fundamental ($N = 1$) peak of the magnetoimpurity resonance in n-GaAs the time τ_{2p_-} decreases more than by an order of magnitude], the value $\delta\tau^e$ is close to the lifetime τ^e of the excited donor out of resonance. The value τ^e is inversely proportional to the carrier concentration n. Since the probability v_{1f} is proportional to the generation rate, the product $v_{1f}\tau^e$ and, hence, the value $\delta n/n$ in eq. (33) appears to be independent of the generation rate.

The temperature dependence of the oscillation amplitude can be also easily explained in the framework of the model suggested. Indeed, temperature changes in the region $kT \ll E_{ion}^d$ should not affect the concentration of hot electrons and, consequently, the value v_{1f}. However, since most of the electrons are thermalized, their overall concentration increases with T due to the decrease of the recombination probability. Therefore τ^e should decrease with increasing T, and, in accordance with eq. (33), the relative resonant amplitude should also decrease, as it was observed by Zverev and Shovkun (1984a).

Now we proceed to the additional resonances in n-GaAs (fig. 4). They have the same form as the main resonance $2p_- - 1s$. This indicates that they are also caused by transitions to the ground state from the excited donor states with numbers 2, 3, ... situated between the levels 1 and f. The set of concentrations $n = N_f, ..., N_3, N_2, N_1, N_0$ is to a great degree determined by the bottleneck $1 \to 0$ in the chain of transitions $f \to ... \to 3 \to 2 \to 1 \to 0$. Above we have considered the case, when the resonance broadens this bottleneck. It is easy to see, however, that a resembling shift of equilibrium can be achieved by switching on the resonant by-pass $(2 \to 0)_{res}$ or $(3 \to 0)_{res}$ from the levels 2 or 3 directly to the ground state. This by-pass is effective, when the frequency of resonant transitions is of the order or higher than the frequency of nonresonant transitions downwards from the corresponding level, i.e., when

$$v_{20}^{res} \gtrsim v_{21}, \quad \text{or} \quad v_{30}^{res} \gtrsim v_{32}.$$

These conditions are more rigid than the condition of the bottle-neck broadening

$$v_{10}^{res} > v_{10},$$

since $v_{10} \ll v_{21}, v_{32}$. As the probability of resonant transitions grows with increasing B, resonances involving higher-lying excited states affect the concentrations N_i and, hence, the transport properties only in strong fields. This explains why additional resonances in n-GaAs are observed only in the range of strong magnetic fields (fig. 4).

5. Inversion of magnetoimpurity resonances

In a number of cases, changes of experimental parameters (the temperature, the intensity of photoexcitation, the magnitude of heating electric field, etc.) cause inversion of magnetoimpurity resonances, namely, transformation of resonant maxima to minima and vice versa. One example of such inversion of magneto-impurity resonances in n-InP, caused by an increase of the electric field, was demonstrated in fig. 10. It is noted in the Introduction that the inversion is not a specific feature of magnetoimpurity resonances, but is inherent to other resonant effects which are registered by the change of the conductivity.

The resonance of any nature can lead to an alteration of both the concentration n_α and the mobility μ_α of the carriers (index α denotes a group of carriers). The sign of the conductivity response

$$\delta\sigma = \sum_\alpha \left(\frac{\partial\sigma}{\partial\mu_\alpha}\delta\mu_\alpha + \frac{\partial\sigma}{\partial n_\alpha}\delta n_\alpha \right)$$

depends on the particular values of parameters. We shall consider for example, a semiconductor with concentrations n of electrons and p of holes, placed in the strong magnetic field ($\mu B/c \gg 1$ both for electrons and holes). The transverse magnetoconductivity $\sigma_\perp = \rho_\perp^{-1}$ for the sample of a finite size

$$\sigma_\perp(B) = ec\eta(B^{-2} + (n-p)^2\eta^{-2}), \qquad \eta = c(n/\mu_n + p/u_p) \tag{34}$$

varies as $\sigma_\perp \propto B^{-2}$ when $B \ll \eta/|n-p|$ and does not vary with B in the fields $B \gg \eta/|n-p|$. The derivatives $\partial\sigma/\partial n$ and $\partial\sigma/\partial p$ change signs during transfer from the region of quadratic increase of the magnetoresistance to the region of its saturation. Therefore, if it is μ that changes in the resonance, then such transfer should inverse the form of the resonance peaks.

It follows from eq. (34) that, when $n \neq p$, in the region of the magneto-resistance saturation the derivatives $\partial\sigma/\partial\mu_n$ and $\partial\sigma/\partial\mu_p$ have opposite signs. If it is the carrier concentrations n, p that change in the resonance, then one can obtain the inversion by altering the initial relation between n and p, for example, by changing the intensity of the photoexcitation.

All these possibilities were analyzed in detail by Gershenzon et al. (1968) on the basis of the cyclotron resonance experiments in p-Ge. In the same paper one more possibility was pointed out which can lead to the inversion in the case of one group of carriers. If alteration of the experimental conditions leads to a change of the carrier scattering mechanism and if the signs of the derivative $\partial\mu/\partial E$ for the 'old' and the 'new' mechanisms are different, then the absorption of the energy δE by carriers in the resonance will lead to the mobility responses $\delta\mu = (\partial\mu/\partial E)\delta E$ of the opposite signs.

All enumerated inversion mechanisms may come into play when the carrier distribution function only feebly differs from the Boltzmann one, though the electron temperature may exceed the bath temperature. Contrary to them, we discuss in this section the inversion which is in principle caused by drastic deviations of the distribution function from the equilibrium one. The inversion of such a type was investigated in detail for the magnetoimpurity resonance in photoexcited p-Ge at liquid helium temperatures (see section 3.3). At these temperatures the equilibrium density of carriers is negligible and all the carriers are those produced by the interband photoexcitation. Their density is determined by the balance of the photoexcitation and the recombination processes and is rather small ($n \approx 10^9$–10^{12} cm^{-3}). Therefore, the distribution function is very sensitive to comparatively weak perturbation.

The inversion of magnetoimpurity resonances in p-Ge proved to be possible when altering the different experimental parameters. Figure 27 demonstrates an example of the inversion when the rate of the interband generation G is altered. The alteration of the electric field $\mathscr{E}$ applied to the sample leads to a similar effect. The critical values of the generation rate G and of the field $\mathscr{E}$ at which the inversion takes place depend on the temperature. Therefore, the inversion can be observed with alteration of the temperature at fixed G and $\mathscr{E}$ values (fig. 28). The relation between G and T values at which the inversion occurs (at fixed $\mathscr{E}$) is shown in fig. 29. It looks like a phase diagram. Increasing of the $\mathscr{E}$ value draws together two branches of the function $G(T)$, especially strongly shifting upwards the lower curve $G_2(T)$. With decreasing $\mathscr{E}$ to the values $\mathscr{E} \lesssim 3$ V/cm, the lower curve shifts downwards to the level $G \approx 10^{14}$–10^{15} cm^{-3} s^{-1} at which the photo-current is very small and oscillations vanish. At intermediate values of $G: G_1 > G > G_2$, the resonances have the form of photocurrent maxima, out of the interval they have the form of minima.

To start with, note that in the ultraquantum limit ($\hbar\Omega \gg kT$) usual electron–electron collisions have no effect on the distribution function. Only if
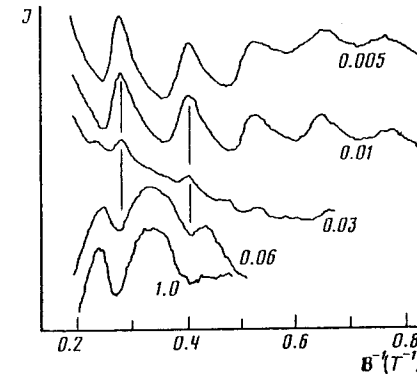

Fig. 27. Inversion of magnetoimpurity oscillations of the photocurrent in p-Ge with changes of the intensity of the interband excitation. The generation rate in 10^{20} cm^{-3} s^{-1} is indicated near the curves. $T = 1.5$ K (after Gantmakher and Zverev 1975).
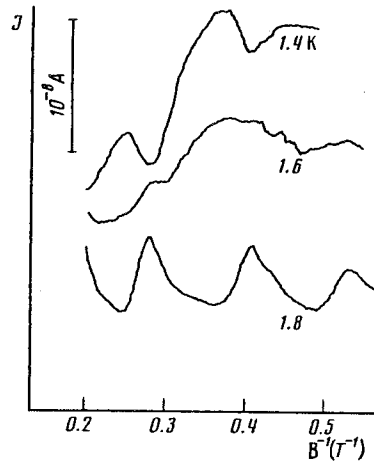
Fig. 28. Inversion of magnetoimpurity oscillations of a photocurrent in p-Ge with changing temperature. The generation rate $G = 2 \times 10^{18}$ cm^{-3} s^{-1} (after Gantmakher and Zverev 1976b).
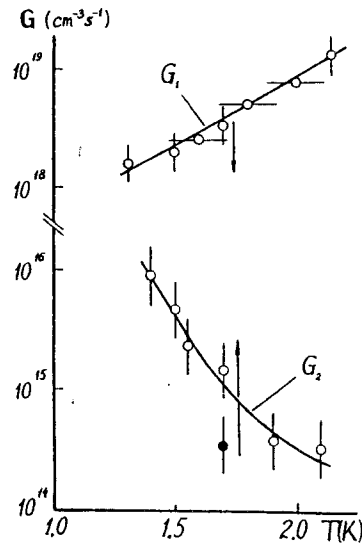

Fig. 29. Connection between the values G and T at which inversion of magnetoimpurity resonances in photoconductivity of p-Ge takes place. The points with vertical error bars were obtained from a series of curves with different G at constant T, while the points with horizontal error bars were obtained with different T at constant G. The $G_1(T)$ curve is plotted at $\mathscr{E} = 5$ V/cm. When $\mathscr{E}$ is increased, it begins to shift in the direction marked by the arrow. The $G_2(T)$ curve is plotted at $\mathscr{E} = 7$ V/cm. Its shift with increasing field is also shown by an arrow. The black point was obtained at $\mathscr{E} = 5$ V/cm.

the collision of two electrons is mediated by a 'third body' (a phonon or an impurity), then it contributes to approaching the Maxwellian distribution. The time for this distribution to establish is (Gantmakher and Levinson 1987)

$$\tau^{-1} = \alpha^{3/2}\tau_{\parallel}^{-1}, \qquad \alpha = n^{1/3}e^2/\kappa kT,$$

where $\tau_{\parallel}$ is the longitudinal momentum relaxation time determined by phonon or impurity scattering. The same relation is valid also for ternary electron collisions, but instead of $\tau_{\parallel}$ one ought to substitute $\tau_{e-e}|_{B=0}$. In the experiments being described, the gas parameter α does not exceed 0.5 even at the highest achieved photocarrier concentration. So the frequency of electron–electron collisions proves to be lower than the other typical scattering frequencies. That is why it is not always possible to ascribe a definite temperature to the electron system.

The results gathered in fig. 29 can be fitted well to a single scheme if the following assumptions are made:

(1) In the region $G_1 > G > G_2$ the distribution function has negative derivative $\partial f/\partial E < 0$ at any energy; the Boltzmann distribution function

$$f(E) = f_0 \exp(-E/kT)$$

is an example. The photoconductivity in this region is 'normal'.

(2) In the regions $G > G_1$ and $G < G_2$ the function $f(E)$ has a segment with positive derivative $\partial f/\partial E > 0$, i.e., with inverse occupancy of states.

In both cases we imply the distribution function of that group of carriers which brings the essential contribution to the conductivity and which is affected by the resonance through changes in the density of carriers, their mobility, etc.

There are two arguments for such a hypothesis. The first is the specific character of the conductivity in crossed magnetic and electric fields in the ultraquantum limit, when all the carriers are in one magnetic subband. The second argument is that one can point to certain physical reasons for an essential distortion of the distribution function along both the curves $G_{1,2}(T)$. We shall discuss these arguments in succession.

The elastic scattering in crossed fields ($\mathscr{E} \perp B$) changes the potential energy of the electron by $e\mathscr{E}\Delta X$, where ΔX is the shift of the center of the cyclotron orbit, which is of the order of the magnetic length $\lambda = (ch/eB)^{1/2}$. Comparison of the energy $e\mathscr{E}\lambda$ and the energy uncertainty $\hbar/\tau$ brings to a critical value of the field

$$\mathscr{E}_{\mathrm{cr}} = \hbar/e\lambda\tau. \tag{35}$$

The field $\mathscr{E} > \mathscr{E}_{\mathrm{cr}}$ is strong and in the scattering the energy conservation law holds

$$e\mathscr{E}\Delta X + \Delta E = 0, \tag{36}$$

where ΔE is the change of the kinetic energy. As the density of states in the magnetic subband $g(E) \propto E^{-1/2}$ is a decreasing function of the energy, for the

electrons with $E > e\mathscr{E}\lambda$ the transitions with $\Delta E < 0$ happen more often than those with $\Delta E > 0$ (Elesin 1968). Therefore the average shift for these electrons is $\overline{\Delta X} > 0$ and their contribution to the current is negative. In the case of the equilibrium distribution function this negative contribution is exceeded by the positive contribution of the electrons near the bottom of the subband in the energy region $E \lesssim e\mathscr{E}\lambda$. Though this energy interval is small, the total number of carriers is large there, so the resulting current is positive.

If the distribution function were $f = \text{const}$, i.e., $T = \infty$, then with eq. (35) being fulfilled the resulting current in the one-dimensional subband would be equal to zero. But if in the energy region $E \approx e\mathscr{E}\lambda$ the derivative $\partial f/\partial E > 0$, then the resulting conductivity can prove to be negative.

Let us return now to fig. 29 and consider the upper curve G_1 of the diagram. The most probable recombination channels are a binding into excitons and electron capture by A^+-centers. Both are the quadratic recombination processes (the latter at not too low temperatures) and the probabilities of both processes increase with decreasing E. Hence, the carriers recombine mainly near the bottom of the band, so that the concentration of the cold carriers is $n_c \propto G^{1/2}$. Meanwhile a number of warm carriers still being cooled is $n_w \propto G$. It is obvious that, as G is increased, at some instant the filling factor of the warm electrons will exceed that of the cold electrons. According to Ladizhinskii (1969) when

$$G > G_1 \approx \tau_c^{-2} \kappa_r^{-1}$$

[τ_c is the cooling time, κ_r the kinetic recombination coefficient associated with the lifetime $\tau_r = (\kappa_r n)^{-1}$] a maximum may arise in the distribution function at the energy value determined by the equation $\tau_c(E) = \tau_r(E)$. From this viewpoint the slope of the upper curve $G_1(T)$ and the effect of the electric field also becomes understandable: both, lowering the temperature and the heating by the electric field, increase the cooling time τ_c.

At low generation rates (curve G_2 in fig. 29) the distortion of distribution function probably takes place entirely at the expense of the electric field. Owing to the large value of $m_\parallel s^2$ (at $B \parallel [100]$ for electrons in Ge $m_\parallel s^2 \approx 1$ K) at helium temperatures the drain to the phonon system of the energy obtained from the electric field is considerably restricted: for electrons with $E < 2m_\parallel s^2$ a phonon emission is hampered while for those with $E < m_\parallel s^2/2$ it is impossible. If owing to the low concentration of excitations the mediated or ternary electron–electron collisions are too rare, then the electric field should cause an effective depletion of the bottom of the magnetic subband.

The inversion of magnetoimpurity oscillations in p-Ge may be observed also by measuring the photoelectromagnetic emf. This effect is shown in fig. 30. Nonequilibrium carriers in these experiments have to diffuse transversely to the magnetic field. Therefore, the distribution of the carriers deep into the sample proves to be nonuniform. This leads to additional complications in the interpretation of the experimental results. Nevertheless, sometimes it is possible
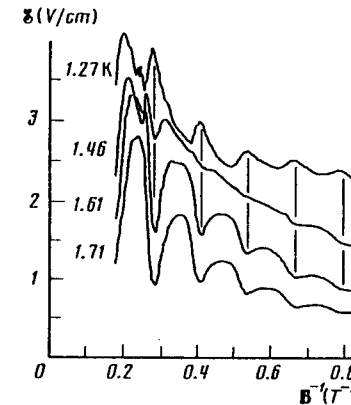
Fig. 30. Inversion of magnetoimpurity resonances of the photoelectromagnetic emf $\mathscr{E}$ with changing temperature (after Gantmakher and Zverev 1975).

to attain a qualitative understanding of the main features of this phenomenon even for this case (Gantmakher and Zverev 1977).

Acknowledgements

References

Aksel'rod, M.M., V.P. Lugovoi, R.V. Pomortsev and I.M. Tsidil'kovskii, 1969, Fiz. Tverd. Tela 11, 113 [Sov. Phys.-Solid State 11, 81].
Aldrich, C., and R.L. Greene, 1979, Phys. Status Solidi b 93, 343.
Altarelli, M., and N.O. Lipari, 1976, Phys. Rev. Lett. 36, 619.
Andreev, S.P., 1978, Zh. Eksp. & Teor. Fiz. 75, 1056 [Sov. Phys.-JETP 48, 532].
Andreev, S.P., 1979, Zh. Eksp. & Teor. Fiz. 77, 1046 [Sov. Phys.-JETP 50, 526].
Ascarelli, G., and S. Rodriguez, 1961, Phys. Rev. 124, 1321.
Bassani, F., G. Iadonisi and B. Preziosi, 1974, Reports on Progress in Physics 37, 1099.
Bogod, Yu.A., V.B. Krasovitskii and S.A. Mironov, 1980, Zh. Eksp. & Teor. Fiz. 78, 1099 [Sov. Phys.-JETP 51].
Boyle, W.S., 1959, J. Phys. Chem. Solids 8, 321.
Boyle, W.S., and A.D. Brailsford, 1957, Phys. Rev. 107, 903.
Boyle, W.S., and R.E. Howard, 1961, J. Phys. Chem. Solids 19, 181.

Brown, R.A., and S. Rodriguez, 1967, Phys. Rev. **153**, 890.

Eaves, L., and J.C. Portal, 1979, J. Phys. C: Solid State Phys. **12**, 2809.

Eaves, L., R.A. Stradling, S. Askenazy, R. Barbaste, G. Garrere, J. Leotin, J.C. Portal and J.P. Ulmet, 1974, J. Phys. C: Solid State Phys. **7**, 1999.

Elesin, V.F., 1968, Zh. Eksp. & Teor. Fiz. **55**, 792 [Sov. Phys.-JETP **28**, 410].

Fisher, P., and H.Y. Fan, 1959, Phys. Rev. Lett. **2**, 456.

Freeth, C.A., P. Fisher and P.E. Simmonds, 1986, Solid State Commun. **60**, 175.

Gantmakher, V.F., and Y.B. Levinson, 1986, Pis'ma Zh. Eksp. & Teor. Fiz. **44**, 532 [JETP Lett. **44**, 687].

Gantmakher, V.F., and Y.B. Levinson, 1987, Carrier Scattering in Metals and Semiconductors (North-Holland, Amsterdam).

Gantmakher, V.F., and V.N. Zverev, 1975, Zh. Eksp. & Teor. Fiz. **69**, 695 [Sov. Phys.-JETP **42**, 352].

Gantmakher, V.F., and V.N. Zverev, 1976a, Zh. Eksp. & Teor. Fiz. **70**, 1891 [Sov. Phys.-JETP **43**, 985].

Gantmakher, V.F., and V.N. Zverev, 1976b, Zh. Eksp. & Teor. Fiz. **71**, 2314 [Sov. Phys.-JETP **44**, 1220].

Gantmakher, V.F., and V.N. Zverev, 1977, Pis'ma Zh. Eksp. & Teor. Fiz. **25**, 44 [JETP Lett. **25**, 39].

Gantmakher, V.F., and V.N. Zverev, 1980, Zh. Eksp. & Teor. Fiz. **79**, 2291 [Sov. Phys.-JETP **52**, 1159].

Gantmakher, V.F., V.N. Zverev, S.V. Meshkov and E.I. Rashba, 1978, Izv. Akad. Nauk SSSR, Ser. Fis. **42**, 1160 [Bulletin of the Acad. of Sciences of the USSR: Phys. Ser.].

Gantmakher, V.F., B.L. Gel'mont, V.N. Zverev and Al.L. Efros, 1983, Zh. Eksp. & Teor. Fiz. **84**, 1129 [Sov. Phys.-JETP **57**, 656].

Gershenzon, E.M., Yu.A. Gurwich, S.L. Orlova and N.G. Ptytsyna, 1968, Proc. 9th Int. Conf. on Physics of Semiconductors (Moscow) p. 286.

Gershenzon, E.M., G.N. Gol'tsman and N.G. Ptytsyna, 1979, Zh. Eksp. & Teor. Fiz. **76**, 711 [Sov. Phys.-JETP **49**, 355].

Gurevich, V.L., 1967, Pis'ma Zh. Eksp. & Teor. Fiz. **5**, 260 [JETP Lett. **5**, 210].

Haller, E.E., and W.L. Hensen, 1974, Solid State Commun. **15**, 687.

Hamagushi, C., T. Shirakawa, T. Yamashita and J. Nakai, 1972, Phys. Rev. Lett. **28**, 1129.

Harper, P.G., J.W. Hodby and R.A. Stradling, 1973, Reports on Progress in Physics **36**, 1.

Hasegawa, H., and R.E. Howard, 1961, J. Phys. Chem. Solids **21**, 179.

Hoult, R.A., 1974, Ph.D. Thesis (University of Oxford).

Instone, T., L. Eaves, J.C. Portal, C. Houlbert, P. Perrier and S. Askenazy, 1977, J. Phys. C: Solid State Phys. **10**, L585.

Ivanov, V.Yu., and T.M. Lifshitz, 1978, Izv. Akad. Nauk SSSR, Ser. Fiz. **42**, 1235 [Bulletin of the Acad. of Sciences of the USSR: Phys. Ser.].

Kaplan, R., 1968, Phys. Rev. Lett. **20**, 329.

Kaplan, R., S.G. Bishop and B.D. McCombe, 1968, Proc. 9th Int. Conf. on Physics of Semiconductors (Moscow) p. 317.

Kikoin, I.K., and S.D. Lasarev, 1967, J. Phys. Chem. Solids **28**, 1237.

Kotera, N., K.F. Komatsubara and E. Yamada, 1966, Proc. 8th Int. Conf. on Physics of Semiconductors (Kyoto) p. 411.

Ladyzhinskii, Yu.P., 1969, Fiz. Tverd. Tela **11**, 2282 [Sov. Phys.-Solid State **11**, 1842].

Landau, L.D., and E.M. Lifshitz, 1977, Quantum Mechanics, par. 133 (Pergamon Press).

Martin, A.D., P. Fisher, C.A. Freeth, E.H. Sabib and P.E. Simmonds, 1983, Phys. Lett. A **99**, 391.

Martin, R.W., H.L. Störmer, W. Rühle and D. Bimberg, 1976, J. Lumin. **12/13**, 645.

Meshkov, S.V., 1979, Fiz. Tverd. Tela **21**, 1114 [Sov. Phys.-Solid State **21**, 647].

Meshkov, S.V., and E.I. Rashba, 1979, Zh. Eksp. & Teor. Fiz. **76**, 2206 [Sov. Phys.-JETP **49**, 1115].

Nakata, H., Y. Ishikawa, E. Otsuka and M. Kobayashi, 1986, J. Phys. Soc. Jpn. **55**, 2859.

Narita, S., 1984, Proc. 1st Int. Conf. on Spectroscopy Shallow Centers Semiconductor (Berkely).

Narita, S., 1985, Solid State Commun. **53**, 1115.

Nicholas, R.J., and R.A. Stradling, 1976, J. Phys. C: Solid State Phys. **9**, 1253.

Nicholas, R.J., and R.A. Stradling, 1978, J. Phys. C: Solid State Phys. **11**, L783.

Palmier, J.E., 1972, Phys. Rev. B **6**, 4557.

Parfen'ev, R.V., I.I. Farbstein and S.S. Shalyt, 1967, Zh. Eksp. & Teor. Fiz. **53**, 1571 [Sov. Phys.-JETP **26**, 906].

Perel', V.I., and D.G. Polyakov, 1981, Fiz. Tekh. Poluprovodn. **15**, 88 [Sov. Phys.-Semicond. **15**, 51].

Pidgeon, C.R., A. Vaas, G.R. Allan, W. Prettl and L. Eaves, 1983, Phys. Rev. Lett. **50**, 1309.

Protasov, E.A., and A.G. Rodionov, 1974, Fiz. Tverd. Tela **16**, 595 [Sov. Phys.-Solid State **16**, 387].

Soepangkat, H.P., and P. Fisher, 1973, Phys. Rev. B **8**, 870.

Tanigushi, M., and S. Narita, 1979, J. Phys. Soc. Jpn. **47**, 1503.

Tokumoto, H., and T. Ishiguro, 1977, Phys. Rev. B **15**, 2099.

von Klitzing, K., 1978, Solid State Electron. **21**, 221.

von Klitzing, K., and G. Landwehr, 1971, Solid State Commun. **9**, 1251.

von Klitzing, K., and J. Tuchendler, 1981, in: Physics in High Magnetic Fields, Solid State Physics, Vol. 24, eds S. Chikazumi and N. Miura (Springer, Berlin) p. 139.

Wallis, R.F., and H.J. Bowlden, 1958, J. Phys. Chem. Solids **7**, 78.

Zverev, V.N., 1977, Fiz. Tverd. Tela **19**, 2015 [Sov. Phys.-Solid State **19**, 1179].

Zverev, V.N., 1978, Pis'ma Zh. Eksp. & Teor. Fiz. **28**, 144 [JETP Lett. **28**, 134].

Zverev, V.N., 1980, Fiz. Tverd. Tela **22**, 3282 [Sov. Phys.-Solid State **22**, 1921].

Zverev, V.N., 1983, Pis'ma Zh. Eksp. & Teor. Fiz. **37**, 89 [JETP Lett. **37**, 109].

Zverev, V.N., and D.V. Shovkun, 1984a, Zh. Eksp. & Teor. Fiz. **87**, 1745 [Sov. Phys.-JETP **60**, 1003].

Zverev, V.N., and D.V. Shovkun, 1984b, Fiz. Tverd. Tela **26**, 356 [Sov. Phys.-Solid State **26**, 212].

Zverev, V.N., and D.V. Shovkun, 1986, Pis'ma Zh. Eksp. & Teor. Fiz. **43**, 379 [JETP Lett. **43**, 488].